L’Institut Agro Rennes-Angers
☐ Site d’Angers ☒ Site de Rennes

Année universitaire : 2024-2025 Spécialité : Ingénieur agronome Spécialisation (et option éventuelle) : Sciences halieutiques et aquacoles (Ecologie halieutique)	**Mémoire de fin d’études** ☒ d'ingénieur de l’Institut Agro Rennes-Angers (Institut national d'enseignement supérieur pour l'agriculture, l'alimentation et l'environnement) ☐ de master de l’Institut Agro Rennes-Angers (Institut national d'enseignement supérieur pour l'agriculture, l'alimentation et l'environnement) ☐ de l’Institut Agro Montpellier (étudiant arrivé en M2) ☐ d’un autre établissement (étudiant arrivé en M2)

A prospective study on the evolution of fisheries’ landings through co-location with energy production in the offshore wind farms of the Gulf of Lion

Par : Louise DANIEL

Soutenu à Rennes le 10/09/2025

Devant le jury composé de :

Président : Olivier LE PAPE

Maître de stage : Stéphanie MAHEVAS

Enseignant référent : Olivier LE PAPE

Autres membres du jury (Nom, Qualité) :

Jean-Eude BEURET (Enseignant-chercheur L’institut Agro Rennes-Angers)

Baptiste ALGLAVE (Maître de conférences Université Bretagne Sud, IUT de Vannes)

Les analyses et les conclusions de ce travail d'étudiant n'engagent que la responsabilité de son auteur et non celle de l’Institut Agro Rennes-Angers

Fiche de confidentialité et de diffusion du mémoire

Confidentialité

☒ Non ☐ Oui si oui : ☐ 1 an ☐ 5 ans ☐ 10 ans

Pendant toute la durée de confidentialité, aucune diffusion du mémoire n'est possible (1).

le 08/09/2025

Date et signature du **maître de stage** (2) : Stéphanie MAHEVAS
(ou de l'étudiant-entrepreneur)

A la fin de la période de confidentialité, sa diffusion est soumise aux règles ci-dessous (droits d'auteur et autorisation de diffusion par l'enseignant à renseigner).

Droits d'auteur

L'auteur(3) Nom Prénom Louise DANIEL
autorise la diffusion de son travail (immédiatement ou à la fin de la période de confidentialité)

☒ Oui ☐ Non

Si oui, il autorise

☐ la diffusion papier du mémoire uniquement(4)

☐ la diffusion papier du mémoire et la diffusion électronique du résumé

☒ la diffusion papier et électronique du mémoire (joindre dans ce cas la fiche de conformité du mémoire numérique et le contrat de diffusion)

(Facultatif) ☐ accepte de placer son mémoire sous licence Creative commons CC-By-Nc-Nd (voir Guide du mémoire Chap 1.4 page 6)

Date et signature de l'**auteur** : le 08/09/2025 Louise DANIEL

Autorisation de diffusion par le responsable de spécialisation ou son représentant

L'enseignant juge le mémoire de qualité suffisante pour être diffusé (immédiatement ou à la fin de la période de confidentialité)

☒ Oui ☐ Non

Si non, seul le titre du mémoire apparaîtra dans les bases de données.
Si oui, il autorise

☐ la diffusion papier du mémoire uniquement(4)

☐ la diffusion papier du mémoire et la diffusion électronique du résumé

☒ la diffusion papier et électronique du mémoire

Date et signature de l'**enseignant** : 10/9/25

(1) L'administration, les enseignants et les différents services de documentation de l'Institut Agro Rennes-Angers s'engagent à respecter cette confidentialité.
(2) Signature et cachet de l'organisme
(3).Auteur = étudiant qui réalise son mémoire de fin d'études
(4) La référence bibliographique (= Nom de l'auteur, titre du mémoire, année de soutenance, diplôme, spécialité et spécialisation/Option)) sera signalée dans les bases de données documentaires sans le résumé

Avant-propos

Utilisation d'une Intelligence Artificielle générative (IAg) pour la rédaction du mémoire

<u>Des outils d'intelligence artificielle générative ont-ils été utilisés ?</u>

☐ Non ☒ Oui

Si oui, préciser pour quels usages :

DeepL traducteur (https://www.deepl.com/fr/translator) et DeepL Write (https://www.deepl.com/fr/write) ont été utilisé pour la traduction en anglais du mémoire et la reformulation de cette traduction.

Acknowledgements

I would like to express my deepest gratitude to my internship supervisor Stéphanie and to my other supervisor who took part in this project, Sophie, Youen, Bertrand and Nolwen. They shared their expertise and advice with me throughout this experience, enabling me to learn and grow during this internship.

I also extend my thanks to the UMR Marbec and the people working there for their welcome, their help and their kindness during my stay with them. In particular, I wish to express my gratitude to Nicolas, whose help and advice on geostatistics was essential during this project. I also thank my fellow interns for their support and sense of humour, which made this experience all the more enjoyable.

My thanks also go to my professors at the Institut Agro who supervised me during my internship and throughout my studies by sharing their knowledge and passion for fisheries and aquaculture sciences.

Finally, I wish to thank my family for their support during moments of joy or doubt, and my friends for their support and strength.

Table of contents

Glossary

COK : Cokriging

CNDP : Commission Nationale du Débat Publique (National Commission of Public Debate)

DIRM : Direction InterRégionale de la Mer (InterRegional Direction for Sea)

FAD : Fish Aggregating Device

GAM : Generalized Additive model

GLM : Generalized Linear Model

LPUE : Landings Per Unit Effort

MEDITS : MEDIterranean Trawl Survey

MW : Mega Watt

OFB : Office Français de la biodiversité (French Office on Biodiversity)

OK : Ordinary Kriging

OP : Organisation de producteurs (Producers Organisation)

OWF : Offshore Wind Farm

PPE : Programme Pluriannuel de l'Energie (Multiannual Energy Programming)

RIC : Réseau Inter Criées (Inter-Auction Network)

SIH : Système d'Information Halieutique (Fishery Information System)

SNBC : Stratégie nationale Bas Carbone (National Low-Carbon Strategy)

VMS : Vessel Monitoring System

VPUE : Value Per Unit Effort

List of figures and tables

List of annexes

1. Introduction

1.1. Offshore wind farms development in France

France has set ambitious targets concerning the development of offshore wind farms (OWF) by aiming for the construction of around 50 OWFs by 2050, which will represent a capacity of 40 GW (speech on the energy state policy by President Macron, 2022). This massive development is part of the National Low-Carbon Strategy (SNBC), which aims to achieve carbon neutrality by 2050 (Ministère de la transition écologique et solidaire, 2020). These objectives are reflected in the Multiannual Energy Programming (PPE), which currently describes the planning calls for projects involving the construction of offshore wind farms up to 2028 (Ministère de la transition écologique et solidaire, 2019).

As part of the public debate “La mer en débat” on maritime spatial planning, which took place from 20 November 2023 to 26 April 2024, priority areas for OWF development by 2050 were mapped (CNDP, 2024a). The Mediterranean coast is expected to accommodate a production between 4 and 7.5 GW. The current configuration plans for five OWF and three pilot farms throughout the Gulf of Lion (Cerema, 2025). The five wind farms projects are named after their location: Narbonnaise, Gulf of Fos, Gulf of Lion Centre, Gulf of Lion East, and Gulf of Lion West and their emplacement is represented on Figure 1, with the corresponding abbreviations that will be used in this report.

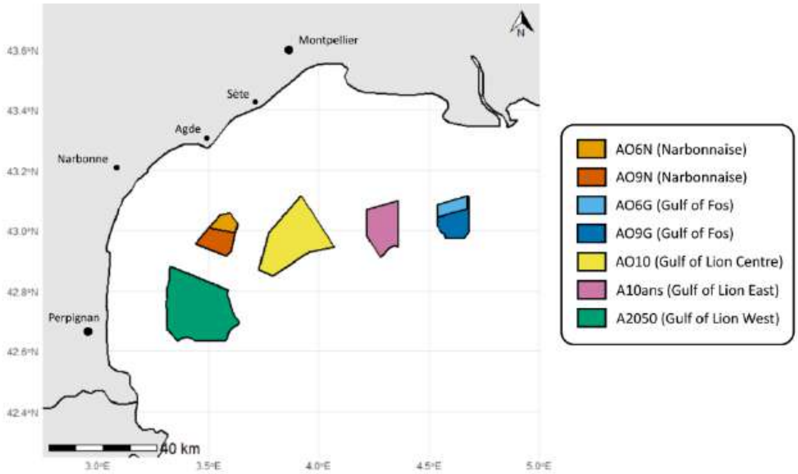

Figure 1: Map of the locations of the future offshore wind farms (OWFs) in the Gulf of Lion

Only one of the pilot farms has been fully constructed and the other two are currently under construction. The construction of the different OWF has yet to begin. The first two projects were awarded to constructors following the tender process AO6 concerning the first part of the Narbonnaise and the Gulf of Fos windfarms. The construction is planned for 2028. The extensions to these parks are currently subject to a call for tenders under AO9 for a total capacity of 750 MW in each OWF. The installation of the Gulf of Lion Centre and East wind farms is planned for the next 10 years. The first will be covered by the AO10 call for tenders, for which the competitive bidding process will be launched in November 2025, with the contract to be awarded in October 2026. The construction of the last OWF is planned for 2050 (Cerema, 2024; Cerema, 2025).

Due to the particular context of the Mediterranean Sea, particularly the deeper seabed near the coast (ranging from 80 to 120 meters) compared to the Atlantic coast and the English Channel, floating wind turbines are preferred over fixed ones (Cerema, 2025). The OWFs will be situated past the 12 miles limit of the territorial waters.

1.2. Impact of offshore wind farms development on existing fisheries

The rapid development of OWF in the Gulf of Lion will affect other activities in the area due to competition for space. Fisheries, in particular, could see their traditional fishing grounds reduced, as they are usually excluded from the vicinity of OWF in Europe for safety reasons (Dupont et al., 2020). This exclusion is systematic during the construction period and often prolonged to the exploitation phase, with some exceptions. For instance, the United Kingdom allows the use of trawls and other bottom-towed fishing gears outside of construction and maintenance periods (Bonsu et al., 2024; Dupont et al., 2020). France also allows fishing within the OWF, but the legislation is different for each park. The parks of Saint-Brieuc and Fécamp allow all types of fishing, including trawling in specific parts, while only the use of static gears is permitted within the Saint-Nazaire park (Ailes Marines, 2024; Eolienne Offshore des Hautes Falaises, 2024; Parc du Banc de Guérande, 2024).

Effort displacement can result from marine space closures, as the existing fishing activities are relocated to other fishing grounds (Alexander et al., 2013; Bonsu et al., 2024; Campbell et al., 2025; Szostek et al. 2025). Even if fishing is possible in the areas, it has been observed that fishers prefer leaving the area mainly motivated by safety concerns (Dunkley and Solandt, 2022; Gray et al., 2016; Hooper et Austen, 2014; Szostek et al. 2025).

The construction of the OWF and the resulting spatial exclusion of fishing activities (through regulation or deliberate avoidance) can have different consequences for the fishing industry. In their report for the European Commission, Dupont et al. (2020) mention the potential loss of revenue resulting from moving to less profitable areas, which may also be accompanied by an increase in cost in fuel caused by increasing distance to fishing grounds. Several studies in the UK interrogating fishers on their perception of these situations have underlined and confirmed the same issues raised by Dupont et al; (2020) (reviewed by Bonsu et al., 2024). The most recent study by Szostek et al. (2025) in the UK reported on the consequences experienced by fishers in the country with the oldest and largest energy production from OWF in Europe. Most of the interrogated fishers reported a negative economic impact of the OWF on their activities linked to effort displacement. They also expect the situation to worsen with the construction of new OWFs, and some are considering leaving the fishing industry if that is the case.

The effort displacement can also have other consequences such as increased competition for space between fishers (Szostek et al., 2025), or a risk of overexploitation of some areas by a “knock-on effect” (Dupont et al. (2020)).

In the French Mediterranean case, the use of trawling gears will be banned in the OWF for safety reasons, since floating turbines do not permit the creation of free corridors in the same way as with a fixed structure do (Jacaud et al., 2015). Trawling is currently the main fishing activity in the areas designated for the OWF construction. This loss of fishing grounds could result in a loss of revenue. The SATHOAN producers' organisation made a first estimation of the loss for the French Mediterranean fishing sector, which would amount to 4 million euros of revenue in a year As an order of magnitude, fishing on the French Mediterranean coast in 2023 represented approximately 14,500 tonnes of landings, worth 92.5 million euros (Ifremer, 2024a). The coastline has 1,108 active vessels, including 1,023 vessels less than 12 m in length, which often engage in several types of fishing, mainly using static gear, and 43 exclusive trawlers (Ifremer, 2024a). The small-scaled fishery, which represents most of the mediterranean fleet usually make one-day fishing trips, which limits their range of action, compared to trawlers who can spend several days at sea (Guyader at al., 2013). This new change in the use of maritime space comes on top of recent restrictions imposed on the sector, notably by the WestMed management plan. According to the European regulation n°2019/1022 of 20 June 2019, the WestMed management plan aims to preserve certain fishery resources such as hake and implements a number of measures, and quotas including spatial and temporal closures of fishing in the Gulf of Lion. These closures directly impact the activity of trawlers. The OWF construction projects come at an already tense time for the fishing industry.

1.3. Co-location as a solution to competition for space between fisheries and OWF

A way to mitigate effort displacement and thus loss of livelihood for fishers is to allow co-location between fisheries and energy production through OWF. Co-location is defined here by the use of a same area by two or more industry, in our case that would be fishing and energy production. Depending on the literature, we can also find the term “co-use” to designate this co-existence between two activities in the same space (Bonsu et al., 2024). The idea behind this principle is to mitigate any losses caused by the implantation of the OWF by according, for example, the access to fisheries or aquaculture projects (e.g. Gonzales et al., 2024; Stockbridge et al., 2025).

In Europe co-location between fisheries and OWF has been studied, encouraged (Guşatu et al., 2022) and even already implemented as we discussed before, but remains largely under documented in terms of technical and economic feasibility especially for floating OWF (Bonsu et al., 2024, De Groot et al., 2014). Most of the studies dedicated to co-location explore the perception of the different stakeholders implicated in these projects. Bonsu et al. (2024) wrote a review of the advantages and disadvantages of such project. It also covers the issues that can arise while implementing this type of activities and recommendations to move forward. One of the main recommendations that surfaced following the different studies to facilitate the co-location is to implicate fishers in the decision process as soon as possible in order to potentially adapt the layout of the OWF, which can influence the space usable by fishing in the area (Bonsu et al., 2024).

The economic feasibility of co-location has been studied in Germany (Stelzenmüller et al., 2021) and the Netherlands with the Win-Wind project (Rozemeijer et al., 2024) for the creation of a pot fishery targeting brown crabs. Both studies concluded that co-location was possible but not economically profitable on its own. Stelzenmüller et al. (2021) has developed a profitable scenario by creating a seasonal fishery during the summer as a diversification of activities for trawlers during their actual least profitable period. In the Netherlands it was concluded that the fishing was technically possible but would necessitate area with a large abundance of crabs and could only sustain a few vessels (Strieman et al., 2023; Rozemeijer et al., 2024). They also mention the possibility to use artificial reefs in order to boost the abundance of targeted species. This idea was also evoked as a solution to sustain crustaceans’ fisheries in the UK (Hooper & Austen 2014; Roach et al., 2018). In France, two research projects are currently underway to understand the socio-economic consequences of the implementation of OWF: EOLENMER (Eolenmer, 2023) and FISHOREMAN (France Energies Marines, 2025).

To the best of my knowledge, all the studies cited above and all the existing co-locations in Europe, only concern fixed OWF and not floating ones. Only one study on the technical feasibility of fishing using traps was found. Wrigth et al. (2023) concluded - after in situ test in the Hywind floating OWF situated in the United Kingdoms - that this type of static fishing gear could be used in co-location with floating OWF.

1.4. Fishwind a project led by the SATHOAN on co-location opportunities in the Gulf of Lion

In the case of the French Mediterranean coast, the construction of OWF will lead to a change in fishing practices in the area by prohibiting the use of the dominant fishing gears, trawls. As a result, and unlike simply reopening the area to fishing, a new activity must be devised and adapted to this context to enable the establishment of a sustainable co-location between fishing and OWF using other fishing gears traditionally reserved for areas closer to the coast.

In order to help establish this new activity, the SATHOAN producers' organisation launched the Fishwind project. The objective of Fishwind is to "explore the interaction between offshore wind farms and artisanal fisheries in order to develop eco-designed solutions to promote biodiversity and blue economy" (OP SATHOAN, 2025). Beyond the co-location of fishing and OWF, the project also aims to create and install artificial reefs to increase biomass for certain species of commercial or ecological interest within the parks. These reefs could thus support fishing in the area while limiting the ecological impact of human activities.

The project is being carried out in partnership with multiple stakeholders, scientific and technical institutes (Ifremer, Cepralmar), fisheries managers and fishers' representatives (CRPMEM Occitanie) and industrial firms (LINEUP OCEAN, 3D CONCRET, BRL Ingénierie). Other public stakeholders (scientists from the University of Montpellier, DIRM, OFB) and private stakeholders (OWF manufacturers) are also invited to take part in the discussions. The project will be carried out in two phases; each divided into four stages (Annex I). The first phase aims to conduct feasibility tests for co-location, design a prototype artificial reef, and begin to develop a future economic model for the commercialisation of reefs. The second phase will involve testing the prototypes at sea and monitoring their environmental impact. Depending on the results, patents will be filed, and a commercial structure will be created to commercialise the artificial reefs.

This study is part of the first stage of phase one. It aims to test the technical and economic feasibility of co-location through the work of a multidisciplinary team, which will carry out sea trials and prospective studies. Four fishing gear types are being considered in the Fishwind project at this stage for co-location: fixed nets, traps and octopus pots, bottom longlines and small surface seines.

1.5. A prospective study on potential catches and revenues in the space destined for OWF construction

The aim of this work is to conduct a prospective study on the potential catches and revenues from fishing activities within the future wind farms in the Gulf of Lion. This report focuses on analyses of two of the four fishing gears considered in the context of this activity: the nets and the traps including the octopus pots. These gears are used by vessels from small-scale fisheries that are less than 18 meters in length. They represent most of the active Mediterranean fleet with 94 % of the 986 active vessels in 2023 (1108 in the vessels in Corse are included (Ifremer, 2024a)). This study focuses on the following question: "What catches and revenues can fishers using these two types of gears expect in the short term in the context of a co-location with OWF, all other things being equal?"

To address this issue, two databases are used. The first is extracted from the fisheries information system of Ifremer (Système d'Informations Halieutiques, SIH). The second is extracted from HALIOP©, an information system set up by the SATHOAN producers' organisation for its members. These two databases provide fishing data at a fine spatial scale on vessels from small-scale fisheries. However, only a small part of the fleet is covered by this data as 913 vessels, out the 986 vessels from small scale fisheries that could operate in the Gulf of Lion, are under 12 meters in length and therefore, are under no obligation to equipe themselves with a VMS-type geolocalisation device (Arrêté du 10 janvier 2012). The data will be used to estimate landings per unit effort (LPUE) in kilogram for different gear-species combination and values per unit effort (LPUE) in euro for each fishing gear, in the Gulf of Lion, particularly within the OWFs. This study represents the first use of HALIOP© for a statistic analysis (Cosnard & Wendling, 2024).

The method chosen to make these estimates is kriging of our spatialized fishing data. This is a geostatistical method of linear estimation. It allows us to take into account spatial correlations and to avoid the assumption of independence between observations contrary to classical generalised linear models (GLM, GAM). This should enable us to obtain a more accurate spatialized estimate. This work follows these steps: 1) LPUE and VPUE observed in the data will be standardised. 2) LPUE for different gear-species combination will be predicted through kriging and then cokriging using covariables such as trawlers' data for the species of interest. 3) VPUE will be predicted for each fishing gear using kriging. 4) Intra-annual variation of VPUE will be explored.

In this report, first the materials and methods used are detailed. Then, the main results of the studies are presented, using the example of four gear-species of commercial interest: monkfish, sole, hake fished by nets and octopus fished by pots. Finally, the results are discussed, the limitations are highlighted and potential improvements to the estimates are proposed.

2. Materials and methods

2.1. Data

2.1.1. Study area

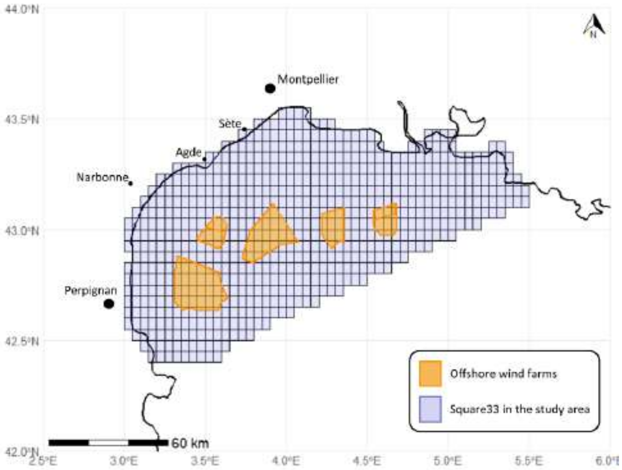

Figure 2: Map of the study area

The study area covers the entirety of the Gulf of Lion, as shown in Figure 2, together with the location of the OWFs. This study area is subdivided in squares of 3 minutes by 3 minutes (0.05°), which represent the scale at which the data is available for this study. The name 'square33' will be used to refer to these subdivisions.

2.1.2. Data used

To carry out this study, we used 2 sources of spatialized fishing data which will be referred to as DB_SACROIS and DB_HALIOP.

2.1.2.1. SACROIS

The Ifremer's Fisheries Information System (SIH) collects information on all fishing vessels of the French fleet. However, precise spatialized data is only available for the vessels using VMS (Vessel Monitoring System). The use of a VMS is mandatory for vessels over 12 metres (length overall), unless an exemption is granted, which is available under certain conditions to vessels under 15 metres since 2012 (Arrêté du 10 janvier 2012). As our study aims to spatially characterize fishing activity, only boats equipped with VMS will be used.

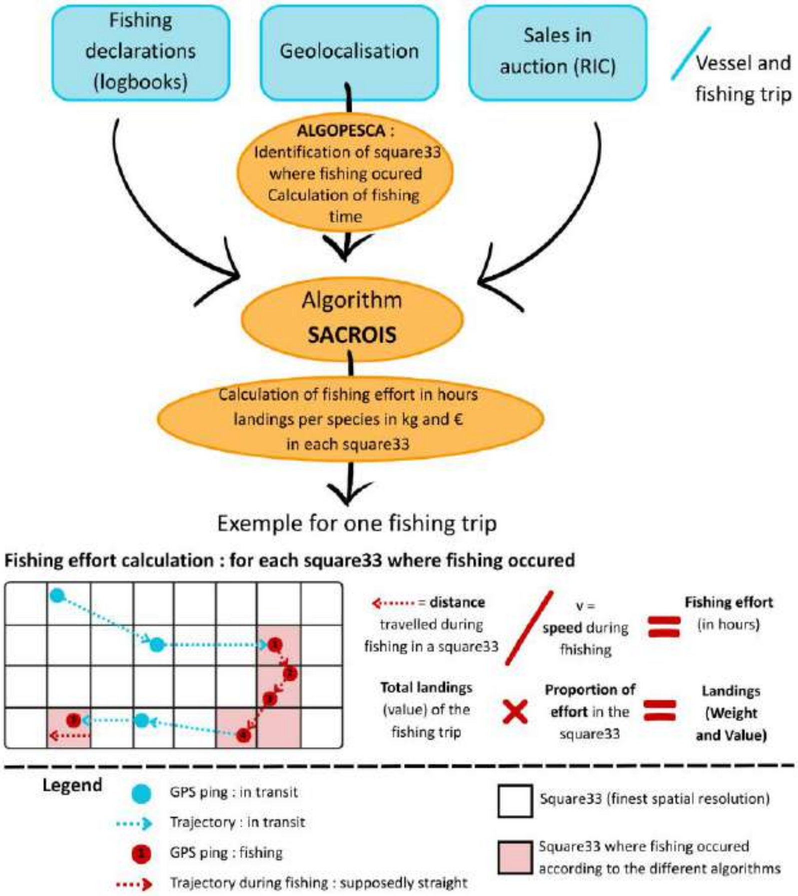

Figure 3: Schematic description of the SACROIS algorithm operation to obtain spatialized fishing data (Ifremer, 2022; Ifremer, 2024b)

The SIH compiles various sources of information using the SACROIS algorithm. To spatialize fishing effort, landings in weight and in euros for each vessel and fishing trip, SACROIS mainly cross-references catch declaration data from logbooks and auction sales data from the RIC (Inter-Auction Network) with the geographical positions of vessels from VMS. Fishing effort (time spent at fishing) is calculated for each square33 according to the ALGOPESCA algorithm assuming fishing with a speed of less than 4.5 knots and a straight line between each vessel ping (Ifremer SIH, 2024b). The landings in weight and value for each fishing trip are then associated with the square33 in proportion to this effort. Figure 3 schematically represents this process.

We therefore have information by vessel, fishing trip, square33, gear, and species for the period 2015 – 2023. The number of vessels in DB_SACROIS dropped gradually between 2015 and 2023 (Annex II).

2.1.2.2. HALIOP

The other source of fishing data is extracted from HALIOP©. It is the fisheries information system of the SATHOAN producers' organisation, which collects fishing data from its members, most of whom are equipped with a geolocation system (VMS, NEMO or other). Information was extracted using the HALIOP© interface for all the gears considered for the co-location and for trawlers.

HALIOP© follows the same general principals as SACROIS with some variations. First, fishing time computation differs slightly from the ALGOPESCA algorithm for gear other than trawls: only the furthest point from the coast where the speed of the vessel was below 4.5 knots is considered as the fishing spot. Second, landings in weight are equally distributed on all the fishing points assuming that the fishing effort was the same across all fishing points during a fishing trip. Third, the value of landings per species is set using the sale data for the trawlers and computed using a mean annual price per kilo for each species for other gears. Fourth, HALIOP© does not aggregate the data by square33. Figure 4 schematically represents this process.

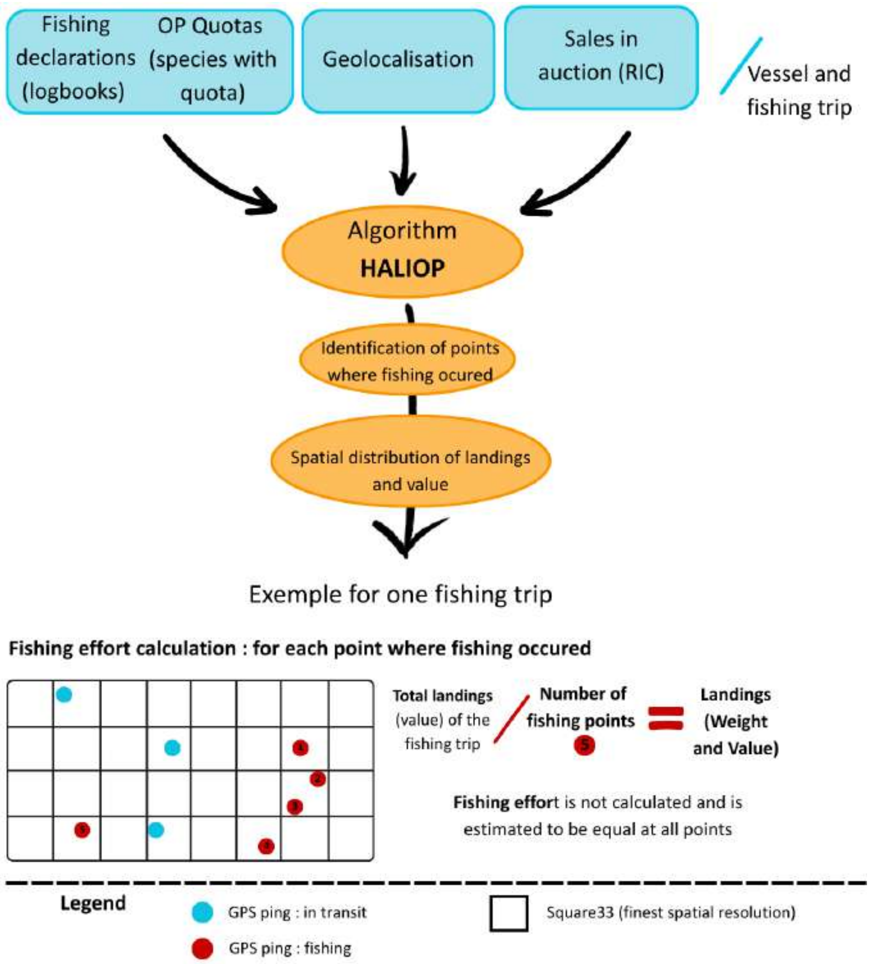

Figure 4: Schematic description of the HALIOP© algorithm operation to obtain spatialized fishing data

We therefore have information by vessel, fishing trip, fishing point, gear, and species for the period between 2017 and 2024. The number of vessels equipped with a geolocation device gradually increased between 2017 and 2023 during HALIOP© development. The number of vessels concerned by co-location in DB_HALIOP increases from 3 to 55 vessels, with less than 15 until 2020 and at least 33 since 2021 (Annex II).

2.1.3. Data treatments

2.1.3.1. Pretreatments on DB_HALIOP

Preliminary processing was necessary before any manipulation of DB_HALIOP data could be carried out. The steps are detailed below and schematised in Figure 5:

- All rows with missing information on species, gear, tonnage or value were removed.
- Some misinformed fishing gears have been corrected based on information from SATHOAN.
- The landings of trawlers were corrected for errors made at auction and transmitted by the RIC, which resulted in negative weights in the data. The correction did not remove all negative weights because no match was found in some cases. In addition, the correction sometimes resulted in outliers with very high prices per kilo (above 90 euros per kilo, which was the maximum) for very low weights (less than 10 grams). Both were deleted, i.e., the negative weights and the outliers. That caused a loss of 0.1% of the landings, all species considered.

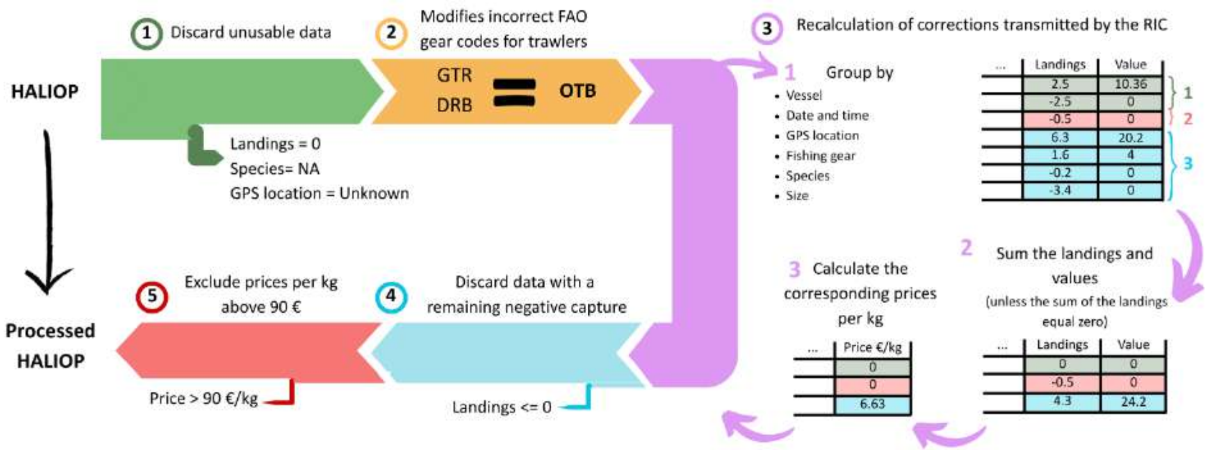

...	Landings	Value	
	2.5	10.36	1
	-2.5	0	1
	-0.5	0	2
	6.3	20.2	3
	1.6	4	3
	-0.2	0	3
	-3.4	0	3

...	Landings	Value
	0	0
	-0.5	0
	4.3	24.2

...	Price €/kg
	0
	0
	6.63

Figure 5: Schematic representation of the data treatments realised on DB_HALIOP

2.1.3.2. Data treatments to fusion the two complementary datasets DB_HALIOP and DB_SACROIS

The objective is to use both datasets together, as they provide complementary information on different parts of the Mediterranean fleet (classes of vessels length, fishing gears and period). DB_SACROIS all vessels over 15 metres in length, including all trawlers, and a large proportion (averaging 78%) of those between 12 and 15 metres. DB_HALIOP contains data on all members of the SATHOAN, which represents around a hundred vessels in the Gulf of Lion, which includes vessels less than 12 meters in length that are not available in DB_SACROIS (between 3 and 55 depending on the year, see Annex II). Therefore, DB_HALIOP includes information on small-scale fishing vessels (vessel under 18 meters), with some using the fishing gears considered for co-location. However, it represents only a small part of these small-scale fisheries, 3.6 % of the vessels average, but 6.5 % in the last two years. They are also complementarity in terms of period covered, since DB_SACROIS only covers the period 2015-2023, while DB_HALIOP covered the period from 2017 to 2024. We created a dataset combining the fishing data available in DB_SACROIS and DB_HALIOP for the fishing gears considered in the context of the co-location. The steps required to create this dataset called are detailed below.

First, we selected only the data concerning the fishing gears considered for the co-location that were located within the study area (Figure 2). Groups of gear types (Annex III) and species (Annex IV) were created to overcome errors in gear declarations or in the identification of certain species. The fishing gear groups retained for co-location, and their appellation are nets (G), traps (FPO), purse seines

(PS), and longlines (LL). The bottom trawlers will be described by the appellation OT. Over the period 2017-2023, for the vessels available in both databases (12 vessels), we chose to prioritize the database that had the longest series (11 in DB_SACROIS and 1 in DB_HALIOP). As indicated above, the computation of fishing effort and the spatial reallocation of landings are not carried out in the same way in the two databases. We therefore need to harmonise the procedure to join DB_SACROIS and DB_HALIOP:

- For the fishing effort, we did not have an accurate measure of fishing time in HALIOP and fishing time for static gears in DB_SACROIS do not reflect reality (Sans & Rodriguez, 2023; Weiss, 2020). We decided to use a similar fishing effort for all fishing trips equal to a fishing day, as small-scale fisheries fishing vessels in the Gulf of Lion operate on a daily basis. For both data sets, a fishing effort of one day was attributed to each fishing trips and equally distributed among the square33 where fishing occurred during each fishing trip (Figure 6).
- Landings in DB_HALIOP were aggregated by square33 to mimic the aggregation in DB_SACROIS. Then, to homogenise the distribution of landings in weight and value, the initial spatial distribution in DB_SACROIS was modified to distribute landings in weight and value equally between the square33 of each fishing trips.
- LPUE (Landings Per Unit of Effort) and VPUE (Value Per Unit of Effort) were derived for each row of this new dataset.

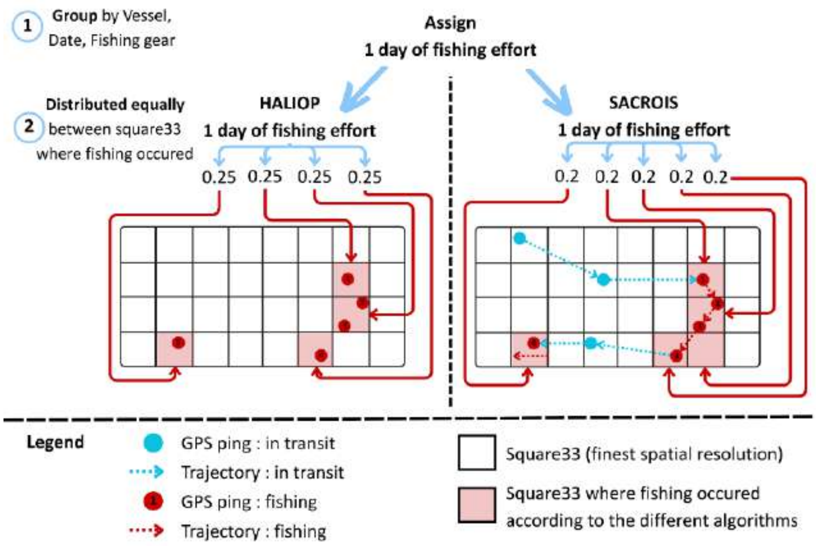

Figure 6: Schematic representation of the harmonisation of fishing effort spatial distribution

The dataset DB_CoACT (see Annex V for its characteristics) contains information on a hundred vessels that performed 10 072 fishing trips in the span of 10 years. The evolution on the number of boats on which we have information is represented in Annex IIB.

DB_CoAct is sparse compared to the entire activity of the vessels declaring using fishing gears of the studied co-location. As described above (section 1.5), most vessels using these gears are less than 12 meters long, and unfortunately, very few are equipped with VMS (or equivalent devices). The percentage of vessels for which we have data compared to the total number of vessels using those fishing gears according to the European vessel registry is summarized by year and types of gears in Annex VI. On average, we have information on 1.3% of vessels using nets, 11.8% of vessels using traps, 5% of the vessels using longlines, and 21.8 % of the vessels using purse seines.

2.1.3.3. Creation of the DB_Trawl dataset: trawlers data from DB_SACROIS in DB_CoAct format

A dataset containing trawler data for the period 2015 to 2023 was extracted from DB_SACROIS, as it contains information on all Mediterranean trawlers (OT), which measure at least 18 metres. LPUE and VPUE by trawler and square33 were calculated by dividing landings in weight and value by effort in fishing hours. This dataset will be used as covariables for our estimations. The dataset has the same format as DB_CoAct (Annex V). It contains information on 87 524 fishing trips in the span of 9 years.

2.1.4. Selection of fishing retained and of the species of interest

2.1.4.1. Fishing gears retained

We chose to focus on two of the fishing gear types considered for co-location: nets and traps. This choice is first based on the quantity and quality of available data and second, constrained by the internship. Nets (G) are the most widely used gear type on the Mediterranean coast, with over 70% of fishers using them (Ifremer, 2024a), but the data in DB_CoAct represent a very small part of this activity. Traps (FP0) were retained because of the importance of octopus fishing in the Mediterranean and the significant amount of data available. Longlines (LL) were discarded because of the limited amount of data we had on the capture of demersal and benthic species, which are of interest in this study. Finally, purse seine fishing was also excluded due to the high variability of its catches linked to the characteristics of its target species, small pelagic fish.

2.1.4.2. Species selected

The two selected gears catch a multitude of species, particularly nets. However, the amount of available data varies between species and does not necessarily allow for a statistical analysis. 21 species were selected, with 8 species fished by both gears and 13 fished only by nets based on three criteria: the tonnage landed, the amount of data available and its spatial coverage of the study area. They are listed below in Table 1, and the number of fishing trips where these species were fished is summarized in Annexe VII.

Table 1 : Species selected for the estimation for each of the fishing gears (species in bold for nets are the species in common with traps)

Fishing gear type	List of species (that were previously grouped) selected
Nets (G)	Sea bass, Brill, **Monkfish**, Capelin, Horse mackerel, **European conger**, Gilt-head bream, Gurnard, **Lobster**, Mackerel, **Hake**, Mullet, Pandora, **Octopus**, **Rays**, Scorpionfish, Goatfish, Catshark, **Cuttlefish**, **Sole**, Turbot
Traps and pots (FPO)	Monkfish, European conger, Hake, Lobster, Octopus, Rays, Cuttlefish, Sole

2.2. Methods

The method chosen, to perform prediction of LPUE per combination of species and fishing gear and VPUE per fishing gear all species combined in the future OWFs, is a geostatistical method called kriging. This method predicts maps accounting for spatial variability. For each combination of retained fishing gear and species for LPUE (Table 1) and each fishing gear for VPUE, 1) LPUE and VPUE data are standardised using generalised linear models (GLM), 2) then used to fit a variogram model describing the spatial structure which 3) will be used to predict maps of LPUE and VPUE through kriging. The detailed steps of the methods and the tools used are presented in this section.

2.2.1. Step 1: LPUE and VPUE standardisation

LPUE and VPUE are not only variables in space but also in time and among vessels. DB_CoAct covers a period of 10 years and comes from different vessels. Therefore, we begin by standardizing LPUE (resp. VPUE), scaling LPUE (resp. VPUE) accounting for temporal and technical differences of both datasets DB_CoAct and DB_Trawl.

We chose to use a generalized linear model (GLM) to standardise the data. Let us call Y the LPUE (resp. VPUE). This model use either a log transformation with a hypothetic normal distribution of the error (lm fitted to log(Y)) or, Y with a logarithm link function and a gamma distribution, constrained by value strictly positive of the LPUE and VPUE. In mathematical terms, this writes, respectively:

$$Y = \hat{Y} + \epsilon = \mathrm{E}[ln(Y)|X] + \varepsilon = A \cdot X + \epsilon \qquad \text{with } \varepsilon \sim N(\mu, \sigma^2) \qquad (1)$$

$$Y = \hat{Y} + \epsilon = e^{E[Y|X]} + \varepsilon = e^{A \cdot X} = \varepsilon \qquad \text{with } \varepsilon \sim \Gamma(\rho, \lambda) \qquad (2)$$

where X stands for some known conditioning variables whose choice is described below, Y represents the LPUE, and A is the vector of the weights associated to each element of $X. A \cdot X$ is thus a linear combination of the explaining variables X which is at the core of the model.

We wanted to account for intra- and interannual variations as well as variation between fishing vessels. For the DB_CoAct dataset we tested the use of different variables to fit our model. The variables MONTH and YEAR were tested to account for intra- and interannual variations. To account for variation between different fishing vessels different technical variables were tested: vessel length, power or gauge and even using the identification of the vessels as the variables.

However, because of the limited number of vessels and very marked difference between the fishing areas between them, the variability explained by technical variables was confused with the spatial variability, which we want to conserve. The spatial variability was also partially confused with the temporal variability as the observation distribution varied between month and year. To avoid losing this spatial variability in the standardised data, an additional qualitive variable was used SQUARE_33, which describes the variability between square33 and thus the spatial variability. This variable was not used to standardize the observations. After this variable was added, none of the variables describing the variation between vessels were kept for the LPUE standardisation in DB_CoAct, as the effect was not significant or the variance analysis detected collinearity. The final variables considered before variables selection in equation (1) and (2) where X = $YEAR + MONTH + SQUARE\_33$.

For DB_Trawl, the problem was not present and therefore the vessel's identification number (NAVS_COD_ANO) was used to account for the variability between the trawlers. The final variables before variables selection in equation (1) and (2) where $X = YEAR + MONTH + NAVS\_COD\_ANO$.

Only the variables that had a significant effect on LPUE (or VPUE) according to an analysis of variance using a Fisher's test (p-value < 0.05) were kept in each model. The analysis of variance was done using the Anova() function of the package "car" (v.3.1.3) of R (v.4.4.2). The choice between the two models (equation 1 or 2) is based on the comparison of the diagnostic of the models' residuals and the fit to the data. The selection for each standardisation model is summarized in Annex VIII.

For the YEAR and MONTH variables, references were chosen for the models. The most recent year for which we have HALIOP and SACROIS data available, 2023, was chosen, except in a few cases where the number of values for that year was very low. For the month variable, the references chosen vary depending on the species, as they are not fished at the same time of year in the OWF area. The reference months chosen, therefore depends on the period of abundance of the species in our areas of interest and the number of observations available. The species were then separated into two groups: those mainly present in summer and those mainly present in winter. The references are summarised in Annex VIII. For the variable NAVS_COD_ANO the average effect of modalities was used as the reference.

Finally, the LPUE and VPUE were standardised using the coefficients estimated by the model for the different modalities of the variables YEAR, MONTH, and NAVS_COD_ANO. Only coefficients significantly different from zero were used in the standardisation, meaning when zero was not within the 95% confidence interval of that value. Thus, the values modified by standardisation will only be those that have a month, year, or vessel significantly different from our references. The formula used to calculate standardised LPUE and VPUE is presented below. Equation 3 relates to DB_CoAct dataset and equation 4 relates to DB_Trawl dataset.

$$LPUE_{standardised} = \frac{LPUE_{observed}}{e^{coef_{YEAR}} e^{coef_{MONTH}}} \quad (3)$$

$$LPUE_{standardised} = \frac{LPUE_{observed}}{e^{coef_{YEAR}} e^{coef_{MONTH}} e^{coef_{NAVS\_COD\_ANO}}} \quad (4)$$

2.2.2. LPUE and VPUE estimations by kriging

The kriging method was chosen to perform spatially explicit estimates of LPUE for the selected gear-species combinations and VPUE for the selected fishing gears in the Gulf of Lion. This geostatistical method of spatial interpolation accounts for spatial correlations that may exist. These estimates are made in several steps. First, a variographic analysis is carried out to define a model describing the spatial autocorrelation between LPUE (or VPUE) observations. This model then enables optimizing the weights used to linearly interpolate between the data. Such an estimate is called a kriging estimate. We used the R package "gstlearn" (v.1.8.0, University MINES Paris-PSL, 2025) to fit all the models.

2.2.2.1. Assumptions

Kriging imposes a second-order stationarity assumption, but avoids the assumption of independence between observations, which we do not have in our case. A second-order stationary assumption implies that for a random field Z of k variables $Z(x_i)$ on k different geographical points x_i for i ∈ {1,k} the first and second moments do not depend on the geographical position of the variable. This implies that:

- The expected value E does not vary with the geographical position:

$$E\big(Z(x_1)\big) = E\big(Z(x_i)\big) = E(Z) \quad \forall\ (i) \in \{1, k\} \quad (5)$$

- The covariance between two variables only depends on the distance h between the two positions and not on their geographical position:

$$cov\Big(Z(x_i), Z\big(x_j\big)\Big) = C_z(h)\ \forall\ (i,j)\ \in \{1,k\} tel\ que\ \big|\, x_i - x_j \big| = h \quad (6)$$

The spatial structure was assumed isotropic, meaning that it is the same in every geographical directions.

2.2.2.2. Transformation of the data to respect kriging requirement on observation position

Before following the different steps to produce LPUE and VPUE estimates, a data transformation is necessary. In fact, kriging fails when observations get duplicates (two values at the same geographical point). In this study we know to which square33 belongs the observation. However, it's precise location in the square33 is unknown and the LPUE is, by default, located at the centre of the square33. Therefore, all observations located in the same square33 are located at the same point. To resolve this problem, two solutions were considered:

- The mean of all the observations in a square33 was used as the only one observation in this square33.
- The observations are scattered on 7 concentric circles around the centroids of each square33. The circles are separated by a distance ε = 0.00005° to ensure that all the data are centred in the square33. In this case the automatic fitting of the variogram was programmed to not considered the pairs of observation at less than a 0.05° of distance to not take into account the random spatial structure created through jitterisation.

Using the averaged data as the advantages of reducing the computation time and smoothing the potential errors of landings distribution as well as the potential residual temporal variability, in particular, when seasonal variations will be explored. However, by doing so we lose all the variability inside the square33 and thus risk underestimating the noise in the models. Moreover, average values calculated with only one or several dozen observations are attributed the same weight in the model, which can skew the estimate if a very high or very low value is isolated. This also violate the statistical assumptions on the variable random field. In contrary the use of jittered data allows us to overcome these drawbacks and to accurately account for the variability in the data. However, for complex models the computation time did not allow for an estimate to be made. Furthermore, the higher noise, potentially due to temporal variations can mask the spatial structure of the data.

Considering the previous points, we will prioritise the use of jittered data when possible. The models using averaged data should be considered with particular caution but will be presented in this work in order to evaluate the capacity of more complex models to improve predictions.

2.2.2.3. Step 2 : Variography

The first step is to fit a variogram model that will describe the spatial autocorrelation between the observations (Aidoo et al., 2015). When the assumption of stationarity is met, the variogram is the total variance minus the covariance as a function of the distance between points (Oliver & Webster, 2014). Both the terms "variogram" and "semivariogram" are often used indiscriminately, the "semi-" usually referrers to the division by two used. We will use the term "variogram" in this work. The variogram is thus rather a measure of the average square among observations at pairs of locations as a function of the distance h (Aidoo et al., 2015; Goovaerts, 1997). To do this, an experimental variogram is calculated from the data using equation 7:

$$\gamma(h) = \frac{1}{2n_h}\sum_{i=1}^{n_h}(z(x_i) - z(y_i))^2 \qquad (7)$$

Where h is the distance between the points x_i and y_i and n_h is the number of pairs separated by h.

Once the experimental variogram has been calculated from the data, a model is fitted to obtain a continuous function describing the variance as a function of the distance between points. Only a limited number of functions can be used, as the function must have "a mathematical expression that guarantees non-negative variances in the predictions" (Oliver & Webster, 2014). The most used and popular structure consists in the combination of the so-called spherical model and a nugget model (Oliver & Webster, 2014). The nugget structure enables to account for variability without spatial structure, the noise. This combination is often used for the estimation of fish abundance for example in Aidoo et al (2015) or Petitgas et al. (2003). These functions were also used in this work combined with a linear structure meant to enable the detection at long distance of spatial structure in the data. The package gstlearn performs automatic fit of the model on the experimental variogram using all or some of the 3 structures selected. The model is fitted by weighted least square (Cressie, 1985). The weights decrease with distance and increase with the number of pairs of observations used to estimate each point of the experimental variogram.

2.2.2.4. Step 3: Kriging: maps of LPUE and VPUE estimates and standard errors

Kriging is used to interpolate, where we have observations, and extrapolate, where we do not, LPUE or VPUE all over the study area. We chose to use ordinary kriging which assumes an unknown constant local average (Goovaerts, 1997).

Estimates are calculated at the centroid of each cell of a grid. Here, a grid covering the entire study area was created, with squared cells of 0.05° to mimic the spatial resolution of our data. Kriging can estimate value where observations are located and provides, in this particular case, the observed value. In all other kriging points, it will provide interpolated values that are a smoothed version of the input variable. To avoid mixing real observations and smoothed interpolated ones in a single map, the grid of estimation is offset by 0.025° compared to the grid with square33 as the observations are associated to the centroid of each square33. For each points an estimate is calculated as a weighted linear combination of the observed values of the variable of interest observed in the moving neighbourhood described by a circle around the point of estimation. Equation 8 describes the expression for each of the points estimated:

$$Z^*(u) = \sum_{i=1}^{n_u} \lambda_i Z(x_i) \qquad (8)$$

Where u is the points to estimate, Z*(u) the estimate by kriging, n_u the number of observations in the neighbourhood used for the estimation, $Z(x_i)$ the observation associated to its kriging weight λi in the estimation.

To have unbiased estimates the sum of the weights must equal 1 : $\sum_{i=1}^{n_u} \lambda_i = 1$ (9). The weights depend on the spatial structure described by the variogram model. Determining the weights is equivalent to solving a system of n_u+1 equations with n_u+1 unknowns, which can be expressed by the following matrix equation:

$A\,.W = B \Leftrightarrow W = A^{-1}.B$ (10), with:

$$A = \begin{bmatrix} \gamma(h_{11}) & \gamma(h_{12}) & \cdots & \gamma(h_{1n_u}) & 1 \\ \gamma(h_{21}) & \ddots & & & \vdots \\ \vdots & & \ddots & & \vdots \\ \gamma(h_{n_u1}) & & & \ddots & 1 \\ 1 & \cdots & \cdots & 1 & 0 \end{bmatrix}, \quad W = \begin{bmatrix} \lambda_1 \\ \lambda_2 \\ \vdots \\ \lambda_{n_u} \\ \lambda \end{bmatrix}, \quad B = \begin{bmatrix} \gamma(h_{1p}) \\ \gamma(h_{2p}) \\ \vdots \\ \gamma(h_{n_up}) \\ 1 \end{bmatrix}$$

Where $\gamma(h_{ij})$ in the (nu+1)x(nu+1) matrix A are variogram values provided by the variogram model for the $n_u * n_u$ distances between the n_u points used for the estimation; $\gamma(h_{ip})$ in matrix B are the values given by the variogram model for the distances between the known points and the point where the estimation is performed; λ_i are the weights whose values are optimized through kriging to ensure the smallest estimation variance; λ is a Lagrange multiplier which is introduced because of the additional degree of freedom induced by the constraint on the weights (equation 9).

The estimation variance is also calculated by:

$$\sigma^2 = W^T.B \qquad (11)$$

Where W^T is the transposed vector of the weights.

Maps of LPUE or VPUE estimates, and standard errors are finally derived. The maps and OWFs estimates that rely heavily on extrapolation should be considered with particular caution, as extrapolating only with data far away from the estimation point is not advisable.

2.2.2.5. Step 4: Global kriging to estimate in OWFs

Estimations of LPUE and VPUE in each of the future OWFs are made using global kriging, which enables us to also calculate the standard error of the estimation for the estimation over an area in its globality. The kriging procedure described above is not relevant to perform the estimation standard error at the scale of the various OWF. The standard error can however be obtained by a global kriging procedure. This is based on spatial integrals that are numerically estimated by gridding the OWF. The numerical approximation is as good as the gird is fine, but this also impacts the computing time. A compromise is thus made between the quality of the approximation and the computing time. For the global kriging, we did not use a moving neighbourhood. All observations were used to calculate estimates in each of the OWFs.

2.2.2.6. Step 5: Cross-validation

Cross-validation is a step enabling comparison between different variogram models. Cross-validation involves removing observations one by one and then re-estimating this value using kriging; it is a leave-one-out validation procedure. The observation and the re-estimated value can then be compared to estimate the model's ability to predict observations. The cross-validation uses the variogram model used for kriging as it is assumed that removing a single observation do not significantly change the model (Goovaerts, 1997).

Different statistics can be calculated using the cross-validation results in order to compare the models. The statistic calculated are:

- The mean cross-validation error: $\frac{1}{n_v}\sum_{i=1}^{n_v}\left(Z(v) - Z^*(v)\right) \qquad (12)$, which is the mean of the prediction errors. Ideally it should be close to 0.
- The mean squared cross-validation error : $\frac{1}{n_v}\sum_{i=1}^{n_v}\left(Z(v) - Z^*(v)\right)^2 \qquad (13)$, which can be compared between models and represent the model capacity to predict the observed values
- The mean squared cross-validation standardized error : $\frac{1}{n_v}\sum_{i=1}^{n_v}\left(\frac{Z(v)-Z^*(v)}{\sigma(v)}\right)^2 \qquad (14)$, which is used to verify whether the standard deviation calculated through kriging is consistent with the observed errors. It should ideally be close to 1, which indicates that the variances are well estimated, and the normality of the residual is respected.

Histograms of the residuals were realised to verify the normality. Plot of the observed values compared to the estimation, and of the residuals as function of the estimation by kriging were also realised to detect bias and evaluate the model prediction capacity.

2.2.3. Model improvement using covariables through cokriging

Kriging provides LPUE estimates for each gear-species combination using landing observations of this combination. However, the amount of available data is quite low, particularly in the areas of future OWFs for which we wish to make an estimate. This is why the confidence intervals of the estimates will probably be large and potentially unusable.

To produce more precise estimates of LPUE, the use of cokriging is tested in this work. Cokriging produces estimates for several variables at the same time while accounting for the covariance between those variables. Therefore, the use of a second variables, whose spatial structure is correlated with the first one can bring additional information, particularly in area where we don't have data on the first variable (Petitgas et al., 2009). Two types of cokriging models were explored. First, we used trawler's data from the DB_trawl dataset for each of the species considered. This covariable covers the entire study area and therefore can bring additional information on areas where the LPUE observation of the gear-species combination was not available.

Then, the use of cokriging is also tested to take into account the covariance between species fished by a same fishing gear. Species can be spatially correlated, for example, if they share a same habitat. According to Petitgas et al. (2009), cokriging can ensure the coherence in the estimated value when variables are linearly related. However, considering the data available the use of a large number of species can render the estimation difficult as we need information on the different variables to be collocated in order to estimate cross-variograms.

Cokriging follow the same general *step as kriging with some variations.*

2.2.3.1. Variography

In multi-variate geostatistics, the spatial structure entails in a mathematically relevant model all the mono-variate spatial structures and all the bivariate structures. A model is fitted on the experimental variogram which now consists of each of the experimental variograms considered before and of experimental cross-variograms between each pair of variables. A multi-variate model of co-regionalization is automatically fitted using the same combination of elementary structures for all the experimental mono and cross-variograms in a row. Experimental cross-variograms are calculated using equation 15:

$$\gamma_{kk'}(h) = \frac{1}{2n_h}\sum_{i=1}^{n_h}(z_k(x_i) - z_k(y_i))\ (z_{k'}(x_i) - z_{k'}(y_i)) \qquad (15)$$

Where h is the distance separating the two points, k is the first variable, k' the second one, x_i and y_i are the two points separated by a distance h.

The above equation indicates that a cross variogram can only be computed for pairs of geographical points where the two different variables are observed. To calculate a cross-variogram the jittered data were paired by day. If several values existed for a same day for a variable the mean of these values was used. This enables us to associate the landings of different species within a single fishing trip and if different vessels fished the same day, it limits the differences in the underlying fish stock.

For each of the tests, the covariables were selected if the cross-variogram revealed the existence of a spatial cross-structure. Covariable which did not resent such a trait were discarded. For the species two basic group were created with winter species and summer species. The classification depends on the reference chosen for the standardisation of the LPUE (Annex VIII).

2.2.3.2. Cokriging (ordinary)

Once the multivariate variogram model is fitted, the estimation through cokriging can be made using the same grid of estimation we defined for kriging. Each point of the grid is estimated by a linear combination of the values of the different variables considered (equation 18).

$$Z_k^*(u) = \sum_{k'=1}^{K} \sum_{i=1}^{n_{k'}(u)} \lambda_{k',i} Z_{k'}(x_i) \qquad (18)$$

Where u is the points to estimate, $Z_k^*(u)$ the estimate of the variable k by cokriging, $n_{k'}(u)$ the number of observations used for the estimation for variable k' at the position u, K is the number of variables considered, $Z_{k',i}(x_i)$ the observation associated to its weight $\lambda_{k',i}$ in the estimation for the variable k.

The weights are then determined according to the multivariate variogram model. The same steps were taken to realise the model cross-validation as for kriging.

2.2.3.3. Global cokriging

An estimation of a mean value and its uncertainty for each of the future OWF could not be calculated through global kriging as it was done for kriging, because of problems in the function used that remained unresolved. Therefore, only the mean was calculated by averaging the value calculated inside each of the OWF area. The standard deviation associated was not calculated.

2.2.4. Exploration of intra-annual variations

The precedent step did not account for intra-annual variability which could be relevant for seasonal migratory species such as the sole (Gaertner et al. 1999) or species for which the abundance in the area linked to seasonality such as hake (Vaz et al., 2023). Due to time constraints, it was not possible to explore the intra-annual variability of LPUE for each gear-species combination. However, the intra-annual variations of VPUE were explored. The analysis could highlight periods of higher VPUE and thus better profitability which could be linked to the variation in species abundance and catchability or to seasonal variations in price, which could be higher during Christmas or during the touristic season for example. We choose to produce an estimation by season. The first season (T1) covers the months of December, January, and February. The second season (T2) covers the months of Mars, April, and May. The third season (T3) covers the months of June, July, and August. The fourth season (T4) covers the months of September, October, and November. This breakdown is based on that of the GOLDYS campaign report (Vaz et al., 2023).

The maps were derived running the kriging procedure described section 2.2.2. using standardized VPUE computed with equation (3) and (4) but removing the Month effect correction. Estimates in each OWF was realised through global kriging and the cross-validation of each model was performed.

3. Results

In this section, we begin by presenting the LPUE spatial estimation results for each of 4 gear-species combinations: monkfish, hake and sole fished by nets and octopus fished by traps, and for both the kriging and cokriging methods. We will also present the results of the VPUE spatial estimation for nets and traps (the value of all species fished by each fishing gear is summed), and of the results on the exploration on temporal variability. In each sub-section, we detail the choice of variograms (step 2), the maps estimated at the Gulf of Lion scale (step 3), the expected averages in the OWFs (step 4), and the quality of the estimates (step 5). The results of the standardisation of LPUE and VPUE will not be commented on but are available in Annex IX.

We presented both results obtained using averaged and jittered data. As said in section 2.2.2.2, the results obtained using averaged data should be considered with caution. The cases where extrapolation was important, should also be considered with caution. Therefore, the estimates from these results are codified using orange contour or font to indicate this. In contrary the other cases will be codified by green.

3.1. Estimation of LPUE spatial distribution in the Gulf of Lion and prediction of LPUE in each OWFs

This section presents the results for the LPUE estimates produced through ordinary kriging (OK), using scattered (models with the title "Jitter") and averaged (models with the title "Mean") standardised LPUE values in DB_CoAct, for each of the for gear-species combination presented. The results for the LPUE estimates produced through cokriging (COK) using the trawlers data of each species in DB_Trawl as covariable in the models. The other cokriging models using LPUE from other species fished by a single gear will not be detailed in the results but are disponible in Annex XI.

For each of our gear-species combination, we will, 1) describe what spatial structure is described by the different models and compare them. Secondly, 2) illustrate the spatial distribution of LPUE obtained using the different models and compare them, 3) report on the prediction made in the OWFs through the use of the different models, and 4) report on the result of the cross-validation and conclude on the use of cokriging to improve the prediction capacity of the model.

3.1.1. Variography: What is the spatial structure of LPUE?

The fitted variograms describing the spatial structure are presented in Figure 7 for kriging models using averaged (first line) and scattered data (second line), and in Figure 8 for cokriging models using averaged data. All the models' characteristics are available in Annex X.

All fitted variogram models show a spatial structure in the data, except for hake when using scattered data (horizontal red line). Apart from this one all models feature a spherical structure with a range of less than 0.5 degrees of distance. For net-hake, net-sole and trap-octopus, the fit of the model to the observations are good for a distance inferior to 1 degree (which represent around 100 kilometres). The goodness of fit of the other models (net-hake, net-sole and trap-octopus with scattered LPUE and net-monkish with both scattered LPUE and mean LPUE) is limited to shorter distances around 0.5 degrees. The observations data points for longer distances are further away from the model curve.

Since the observations used between the two data configurations explored, the resulting models do not describe the same spatial structure. The univariate models using scattered data have higher nugget values for hake, sole and octopus, which is to be expected as the variability at small distance was smoothed by the averaging process of the other data configuration. However, we do not observe this for monkfish where both models do not have a nugget structure.

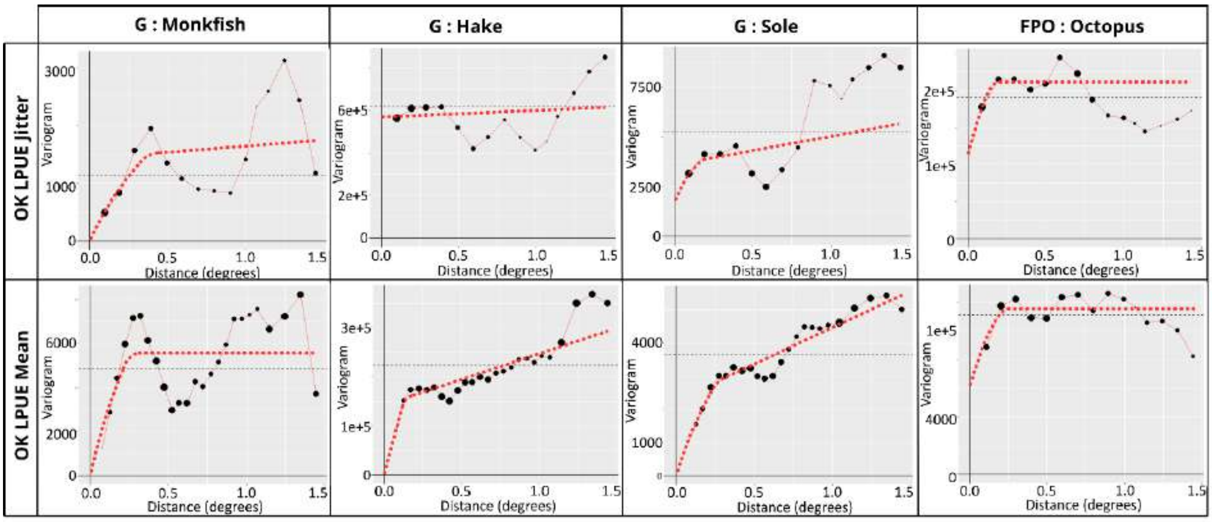

Figure 7: Experimental variograms (black dots with a diameter proportional to the number of pairs used in the calculation) and fitted model (red dotted line) used to produced kriging estimates of monkfish, hake and sole LPUE by nets (G) and octopus LPUE by traps (FPO), using two LPUE configurations of data (averaged by location on the first line, and scattered around the position of origin for the second one). The black dotted line represents the variance of the data.

For multivariate models, the use of a second variable imposes additional constraints on model fitting. As a result, the adjusted models describing the spatial structure of the four gear-species associations considered in the univariate models, using the same data configuration, are altered. The model for net-sole is virtually identical. The ones for net-monkfish and net-hake are similar but have a higher nugget value. However, the model for trap-octopus shows differences with a significantly very larger range for the spherical structure.

The latter model is also the furthest from the data and does not seem to describe the spatial structure of LPUE for octopus caught with pots or trawls satisfactorily. The models for net-monkfish, net-hake, and net-sole show similar adjustments to the data as the univariate models. The adjustment of the models to the trawler LPUE data for each of these three species is satisfactory up to a distance of approximately 0.5 degrees.

The spatial covariance between the two variables is described by the last graphs at the bottom left. We can observe a spatial structure with a positive correlation between the LPUE of nets and trawlers for monkfish, sole, and, to a lesser extent, octopus, but this correlation is not marked for hake.

Considering these results, two conclusions can be drawn. Firstly, the use of the cokriging model to predict the LPUE of octopus by traps is not recommended due to the unsatisfactory fit to the data of the model. Similarly, the use of the cokriging model to predict the LPUE of hake by nets is not very useful due to the low spatial covariance between the two variables in the model. Secondly, for the kriging and cokriging procedure, it is preferable to use a moving neighbourhood of 0.5° (approximately 50 kilometres) in order to use the models only for distances where they are well adjusted to the data and to keep a neighbourhood slightly larger than the range of the models.

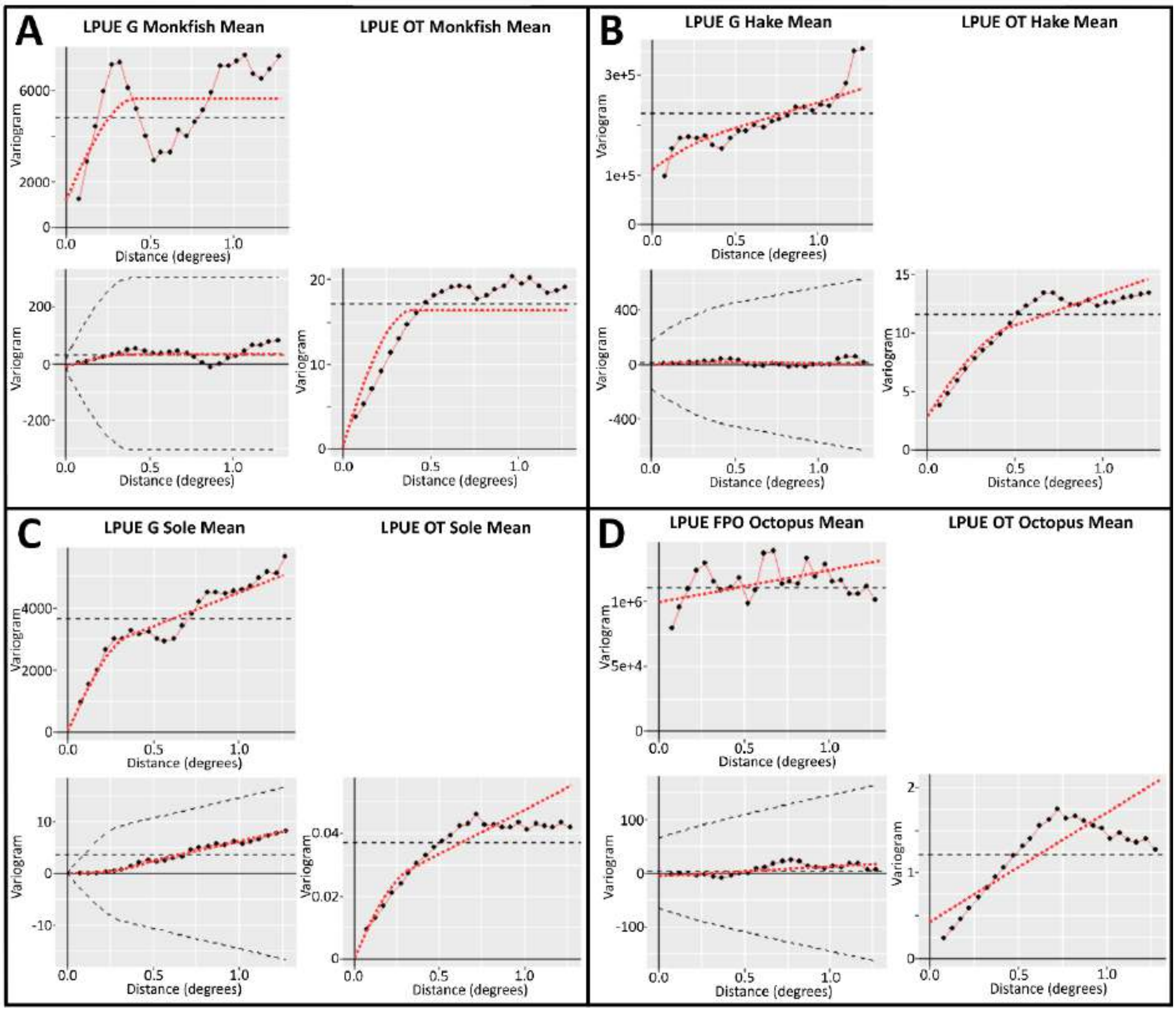

Figure 8 : Experimental cross-variograms (black dots) and fitted models (red dotted curve) used to produced cokriging estimates : A: of monkfish LPUE by nets (G),B: of hake LPUE by nets, C of sole LPUE by nets, and D: of octopus LPUE by traps (FPO), using averaged data by location. In each cross-variogram, the top left plot is the univariate variogram for the gear-species combination of interest, the bottom right plot is the univariate variogram of the second variable, which is the concerned species LPUE by trawls (OT), the bottom left plot is the cross-variogram of the two precedent variables. The black dotted line represents the variance of the data.

3.1.2. Maps of kriged LPUE: What is the LPUE spatial distribution in the Gulf of Lion?

Based on the selected variogram model for each combination gear-species, we produced LPUE estimates at the scale of the Gulf of Lion through kriging for the two univariate models and cokriging for the last one (Figure 9). For a gear-species (in column), we use the same scale to compare the estimates from the three methods.

For all combination of gear-species, all methods identify the same area of high and low LPUE and produce estimates in the same order of magnitude. The LPUE estimates produced with scattered data for hake and sole are spread over a narrower range, with lower maximum values, than the ones produced with averaged data. This is linked to the higher nugget values for both of this models that were described in section 3.1.1. Similarly, the LPUE estimates for net-monkfish, net-hake and trap-octopus obtained through cokriging present the same characteristics. The resulting estimates are smoother for a variogram model, when the spatial structure is less pronounced.

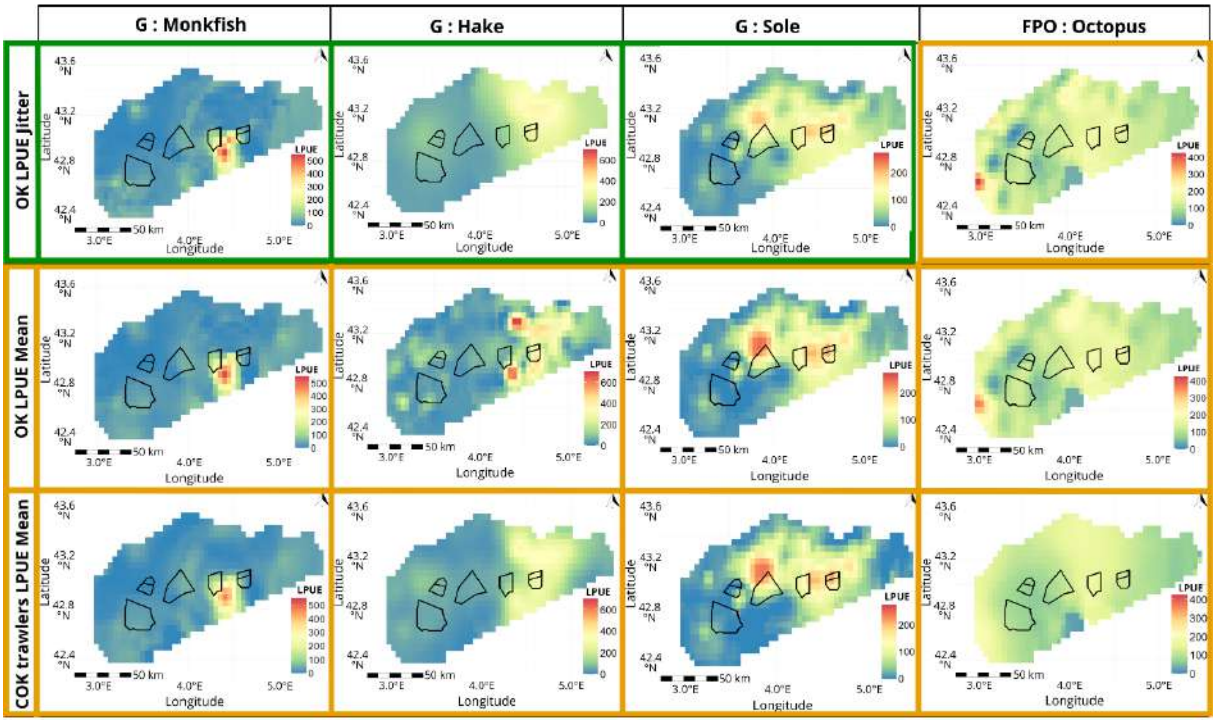

Figure 9 : Maps of the LPUE (in kg/day) estimates in the Gulf of Lion monkfish, hake and sole LPUE by nets (G) and for octopus LPUE by traps (FPO) using kriging on scattered data (first line), or on averaged data (second line), or using cokriging on average data using LPUE from trawlers as covariable (third line). Each column contains the LPUE estimation for the gear-species combination described using the three different models. The scale for LPUE estimates is consistent in a column. Maps with the orange outline are very uncertain as the models used violates some of the hypotheses and thus should be used with caution.

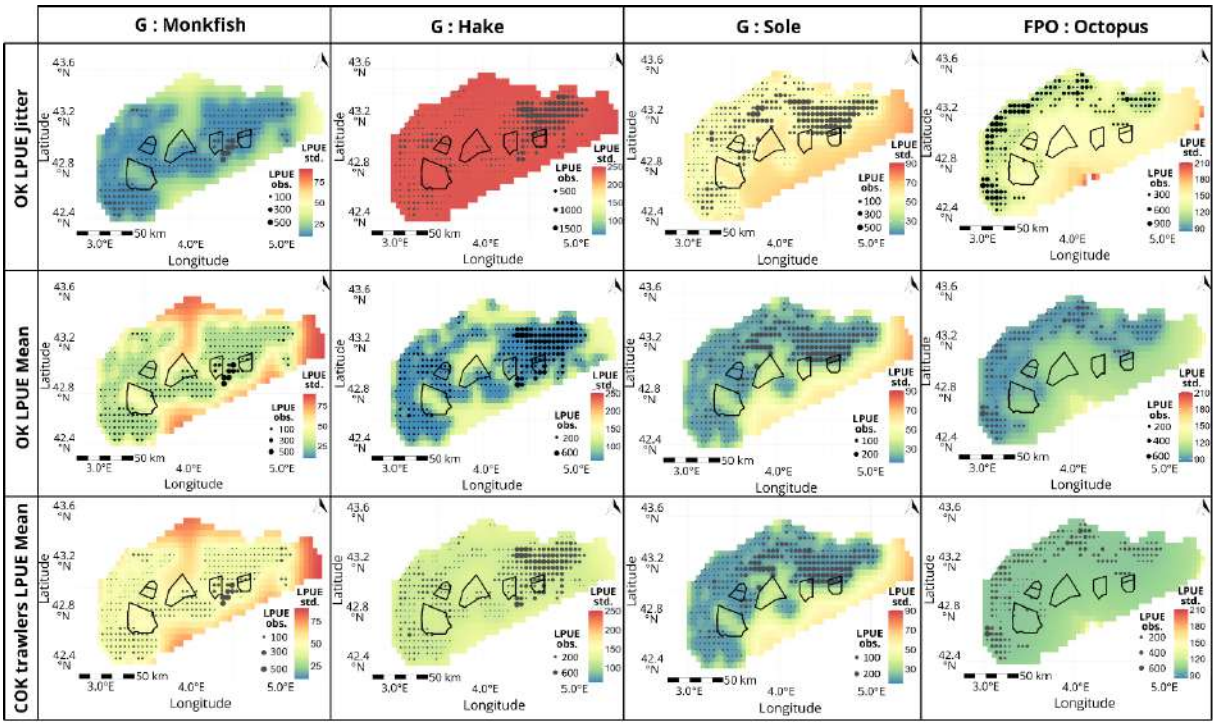

Figure 10 : Maps of the LPUE standard deviation (LPUE std.) in the Gulf of Lion monkfish, hake and sole LPUE by nets (G) and for octopus LPUE by traps (FPO) using kriging on scattered data (first line), or on averaged data (second line), or using cokriging on average data using LPUE from trawlers as covariable (third line). Each column contains the LPUE std. for the gear-species combination described using the three different models. The scale for LPUE standard deviation is consistent in a column.

For net-monkfish, one area of high LPUE has been identified further offshore, close to two future OWFs: the Gulf of Fos and the Gulf of Lion East. For net-hake, the eastern part of the Gulf of Lion hosts the highest LPUE estimates, with an area extending from the coast near the mouth of the Rhône to the continental shelf border. This area includes the same OWF areas as for net-monkfish. Net-Sole is characterised by high LPUE in the eastern half of the gulf at intermediate depths, a geographical area including three of the OWF areas (Gulf of Fos, Gulf of Lion East and Gulf of Lion Centre). Finally, the LPUE of trap-octopus are the highest on the west coast and show similar values in the rest of the Gulf. This difference is less marked for the cokriging estimates but as said before the cross-variogram model quality used in this estimation is lower.

The kriging standard deviation (LPUE std.) are presented in Figure 10. In general, i.e., when the variogram departs from a pure nugget effect, uncertainty increases as the distance between the estimation point and the data location increases. This is one of the reasons why estimates extrapolated far from the variable's observation areas should be treated with caution. Here, all the estimations for trap-octopus LPUE are concerned by this precaution.

Standard deviation values are higher for estimates made using jittered data, except for net-monkfish. The higher uncertainty is partially explained by the higher variance in the observations that was not smoothed by averaging and the higher nugget values for these three gear-species combinations. Moreover, the estimates' uncertainties for hake using jittered data are spatially homogenous because of the variogram model structure (nearly a pure nugget effect). Similarly, the higher nugget effect resulted in higher standard deviation for the cokriging estimations for net-monkfish, net-hake, and trap-octopus.

3.1.3. Predictions of LPUE in OWFs: What LPUE are estimated for each OWFs?

The mean LPUE estimate across each OWF area and the confidence interval at 95% (assuming a gaussian distribution) are presented in Table 1. The LPUE estimates in each OWF are very similar from one model to another for all species and their confidence intervals overlap, except for net-monkfish except for the estimation in the Gulf of Lion East (A10ans) for monkfish, where the highest LPUE is estimated and for A06N and A09N for which there is an order of magnitude of difference in the estimates to the detriment of the procedure based on the mean data. Most of the estimations present large confidence intervals which sometimes include a null LPUE. Confidence intervals could not be calculated for the cokriging estimations (see section 2.2.3.3).

As previously emphasised, the OWF Gulf of Fos (AO6G and AO9G) and the Gulf of Lion East (A10E) have the highest LPUE estimations for all species. The lowest LPUE values are found in the OWF Narbonnaise (AO6N and AO9N). The high estimated LPUE values are coherent with the observed LPUE values around these areas (Figure 10). However, we cannot assess this for octopus as, it is the worst-case scenario regarding the estimation of LPUE in the various OWFs. The data on which the estimation procedure is based are coastal and none of the OWFs get inner data. All the octopus' estimations in the OWFs are thus issued from the extrapolation of data with a model that is itself extrapolated from coastal to offshore areas (stationary hypothesis). These cases probably exceed the threshold of realism in the use of the model.

Following the reflexion on the problematic use of the averaged data (see section 2.2.2.2), the use of estimates from kriging models using jittered data is recommended.

Table 2: LPUE (in kg/day) estimates in each of the future OWF areas for all the cases considered for the gear-species combinations net-monkfish, net-hake, net-sole, and trap-octopus. The different OWF are described by their abbreviation. Confidence intervals at 95% are in brackets below the estimate when available. The numbers in orange cells should be considered with caution.

	AO6N	AO6G	AO9N	AO9G	AO10	A10ans	A2050
Monkfish G							
jitter	**28.7** (0 - 101.8)	**41.7** (0 - 114.5)	**29** (0 - 99.9)	**42.9** (0 - 114.5)	**34.7** (0 - 97.3)	**44.1** (0 - 112.9)	**31.5** (0 - 93)
mean	1.6 (0 - 21.6)	34.9 (16.8 - 53.1)	2.9 (0 - 17.6)	38.6 (11.8 - 65.5)	28 (0 - 60.7)	142 (121.9 - 162.1)	32.2 (0 - 67.2)
COK	1.8	44.4	4.4	53.5	31.4	170.7	32.1
Hake G							
jitter	**80.5** (37.2 - 123.8)	**268.3** (236.2 - 300.4)	**82.8** (43.1 - 122.6)	**246.7** (208 - 285.4)	**54.7** (10.1 - 99.4)	**112.3** (72.9 - 151.7)	**62** (26.7 - 97.4)
mean	68.8 (10.8 - 126.3)	264.3 (213.5 - 315)	67.6 (15.9 - 119.2)	265.7 (213.8 - 317.6)	42.2 (0 - 98.4)	119.4 (66.7 - 172)	51.2 (0.2 - 102.1)
COK	71.9	258.4	70.8	265.7	50.8	123.1	50.6
Sole G							
jitter	**42.7** (0 - 120.8)	**110** (33 - 187.1)	**36** (0 - 108)	**108.8** (33.4 - 184.2)	**73.4** (17.5 - 129.4)	**99.1** (30.5 - 167.7)	**22.3** (0 - 73.3)
mean	38.4 (0 - 131.6)	104.9 (11.7 - 198.2)	35.5 (0 - 124.4)	102.2 (9.5 - 195.0)	73 (0 - 148.1)	95.1 (8.2 - 182.0)	18.6 (0 - 90.1)
COK	14.2	187.5	15.5	167.4	108.3	129.9	8
Octopus FPO							
jitter	105.8 (0 - 256.2)	159.4 (31.7 - 287.2)	128.9 (4.6 - 253.1)	141.4 (0 - 287.3)	128.9 (19.3 - 238.6)	130.2 (0 - 268.7)	115.9 (27.9 - 203.9)
mean	94.9 (0 - 201.2)	161.6 (69.3 - 254.0)	110 (20.2 - 199.8)	148.4 (39.2 - 257.7)	125.4 (32.1 - 218.7)	130 (18.1 - 183.4)	112.2 (41.0 - 183.4)
COK	71.9	122.5	68.3	117.2	96.9	156.4	81.2

3.1.4. Cross-validation: What model should preferably be used?

Table 3 presents a set of model quality indicators obtained for each model through cross-validation. Those indicators are used to compare, first, the accuracy and the precision of the kriging estimation in the configuration of averaged LPUE versus scattered LPUE. Then, the kriging and cokriging estimations using averaged data will be compared.

Concerning the two kriging models, the mean prediction error is low for all the models tested. It is slightly higher for models using scattered data net-monkfish and net-hake, and in the contrary a bit lower for the two other gear-species combinations. All mean squared standardised errors should be close to 1. The value of this indicator is further away from one for all the kriging models using scattered data than the kriging models using averaged data. Particularly, for net-monkfish which present a value significantly higher than all the models that were tested. This would mean that this models highly underestimates the uncertainty, which is problematic to realise predictions. The mean squared prediction error cannot be compared between these two models as different data were used.

For the comparison between kriging and cokriging using averaged data, we can observe that cokriging models have a lower mean prediction error, except for net-hake, but all values are close to zero indicating unbiased estimates. The mean squared prediction error, which describes the model fit to the data, is higher for cokriging for net-monkfish and trap-octopus, but lower for net-hake. The value for net-sole is comparable between the two models. The mean squared standardized error of both models are similar for all gear-species combination, but slightly further away from one for the cokriging models, except for trap-octopus where they are equal.

To conclude on the comparison between kriging models using two different data configurations, it is preferable to use jittered data even if its indicators are less favourable for the reasons mentioned above. This applies to all gear-species combination, except potentially the model for net-monkfish.

The use of a cokriging model did not yield the expected improvement for LPUE prediction. However, the cokriging models are comparable to kriging models and sometimes slightly better (net-sole model). This opens other possibilities, such as exploring the use of additional covariables or performing cokriging using jittered data to improve the models.

Table 3: Cross-validation statistics for the LPUE estimation through ordinary kriging (OK) using two configuration of data, scattered (jitter), and averaged(mean), and through cokriging (COK) with trawlers' data (OT), for the gear-species combination net-monkfish, net-hake net-sole and trap-octopus.

Model	Mean prediction error	Mean squared prediction error	Mean squared standardized error
OK G Monkfish jitter	-0.13	693	857.19
OK G Monkfish mean	0.05	993	0.80
COK G OT Monkfish mean	-0.02	1184	0.56
OK G Hake jitter	1.65	40850	0.71
OK G Hake mean	0.33	9931	0.77
COK G OT Hake mean	0.72	8982	0.68
OK G Sole jitter	0.03	3189	1.77
OK G Sole mean	0.16	771	1.23
COK G OT Sole mean	0.02	768	1.34
OK FPO Octopus jitter	-0.08	16399	1.44
OK FPO Octopus mean	-0.63	7792	0.89
COK G OT Octopus mean	0.21	9373	0.89

3.2. VPUE estimates and their temporal variations

3.2.1. Estimation of VPUE spatial distribution in the Gulf of Lion and VPUE prediction in the OWFs for traps and nets

This section presents the results of the VPUE estimation for nets (G) and traps (FPO) using averaged or jittered data. The spatial structure is explored. Then maps of the estimated VPUE and the associated kriging standard deviation are presented. Estimates in each OWFs for both gears are summarised and finally the results from the cross-validation of the models are developed.

3.2.1.1. Variography: What is the spatial structure of VPUE?

For nets and traps, the variogram models (Figure 11) fit the data well in both data configurations (mean and jitter) for distances of at least 0.5 degree and provide similar spatial structures (same range). However, the spatial structures are more pronounced (smaller proportion of nugget) when averaged data are used. The moving neighbourhood is set to 0.5 degrees (around 50 km), following the same reasoning as for LPUE.

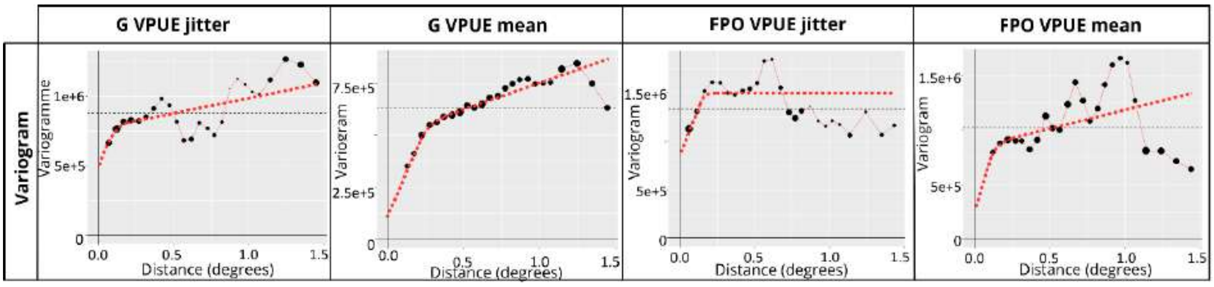

Figure 11 : Experimental variograms (black dots with a diameter proportional to the number of pairs used in the calculation) and fitted model (red dotted line) used to produced kriging estimates of nets (G) and traps(FPO) VPUE, using two LPUE configurations of data (averaged by location called "mean", and scattered around the position of origin called "jitter"). The black dotted line represents the variance of the data.

3.2.1.2. Maps of kriged VPUE: What is the VPUE spatial distribution in the Gulf of Lion?

The VPUE estimates (in euros/day) all species considered for nets (G) and traps (FPO) in the Gulf of Lion, using averaged and scattered data, are mapped with their associated estimates of standard deviation (resp. first and second rows in Figure 12, using the same scale between the different data configurations). The VPUE estimated by the models using jittered data present a smaller range of estimated value which can be linked to the more important nugget effects in the variogram models that were used (Figure 11).

For traps and nets the models using averaged and scattered data provides similar spatial patterns of VPUE.

For nets, the areas with the highest estimated VPUE are located in the centre and the eastern half of the gulf, which corresponds to the areas with the highest estimated LPUE for the three species we presented.

For traps, one of the areas with the highest VPUE estimations is located near the western coast and coincide with high estimated LPUE value for octopus. However, the other high VPUE area further offshore was not identified as a hotspot for octopus catches.

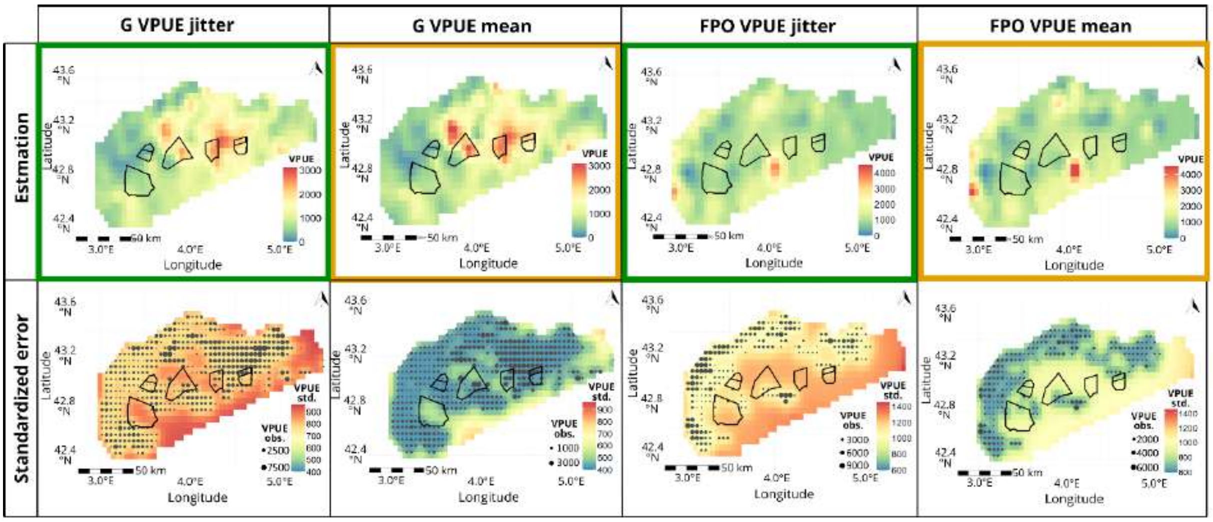

Figure 12: Maps of the VPUE (in euros/day) estimates and standard deviations (VPUE std.) in the Gulf of Lion obtained by kriging for nets (G) and traps (FPO) using averaged (mean) and scattered data (jitter). The OWF areas are represented by a black contour and the observations by black dots (VPUE obs. in euros/day. The maps in orange should be used with cautions.

The data coverage for nets includes all the OWF areas and cover most of the gulf area, which avoid high uncertainties in the OWF. However, for traps there is a lack of data in the OWF areas, which are therefore characterised by a higher uncertainty than on the coast. The standard deviation is higher when scattered data are used.

3.2.1.3. Predictions of VPUE in OWFs: What VPUE are estimated for each OWFs?

The VPUE estimates for each OWF (Table 4) have wide large confidence intervals, which are narrower for the estimations realised using jittered data. For nets, the highest VPUE estimates are in the OWF Gulf of Fos (AO6G and AO9G), the Gulf of Lion Centre (AO10) and Gulf of Lion East (A10ans). Their value is estimated between 1200 to 1700 euro for a day of fishing in the area. For traps, VPUE estimates are similar in all the OWF and are around 1000 euros a day.

Table 4: VPUE (in euros/day) estimates in each of the future OWF areas for nets (G) and traps (FPO) using averaged (mean) and scattered data (jitter). The different OWF are described by their abbreviation. Confidence intervals at 95% are in brackets below the estimate. This estimates in orange should be considered with caution.

	AO6N	AO6G	AO9N	AO9G	AO10	A10ans	A2050
G VPUE							
jitter	**759** (0 - 1678)	**1629** (745 - 2513)	**706** (0 - 1545)	**1583** (738 - 2428)	**1238** (625 - 1851)	**1713** (947 - 2479)	**732** (155 - 1308)
mean	**786** (0 - 2007)	**1407** (204 - 2611)	**777** (0 - 1948)	**1343** (165 - 2523)	**1181** (190 - 2173)	**1485** (360 - 2611)	**737** (0 - 1698)
FPO VPUE							
jitter	**1149.8** (0 - 2337.9)	**1139.9** (108 - 2171)	**1234.8** (247 - 2222)	**1170.1** (0 - 2371)	**1049.9** (265 - 1835)	**1147** (0 - 2321)	**1076.7** (316 - 1837)
mean	**1037.7** (0 - 2415)	**1088.9** (0 - 2446)	**1056** (0 - 2316)	**1124.1** (0 - 2447)	**1236.6** (272 - 2201)	**1304.3** (97 - 2511)	**1158.6** (271 - 2046)

3.2.1.4. Cross-validation: Comparison between models and model selection

The cross-validation statistics (Table 6) indicates the models present relatively small mean prediction errors, with the models using jittered data performing slightly better. Overall, according to these statistics, for nets, the model using jittered data performs better. For traps the distinction is less clear as the model using averaged data has a mean standardised error closer to 1 than the jittered model.

Table 5: Cross-validation statistics for the VPUE estimates made with ordinary kriging (OK) for nets (G) and traps (FPO) using averaged (mean) and scattered (jitter) data.

Model	Mean prediction error	Mean squared prediction error	Mean squared standardized error
OK G VPUE mean	1.38	330121	1.47
OK G VPUE jitter	-0.11	364342	1.14
OK FPO VPUE mean	-4.39	684920	1.24
OK FPO VPUE jitter	-0.84	1216893	1.40

The model using scattered data will be preferably used as it is less biased and for the reason explained in section 2.2.2.2.

3.2.2. VPUE temporal variations: Are there seasonal patterns in VPUE estimates?

This section presents the result of the breakdown of the VPUE estimate by season in order to assess the intra-annual variation in revenue. Only the estimates from the models fitted to the averaged data are presented, even though the models selected used scattered data, because of a lack of time. The conclusions and estimates from this should therefore be considered with caution.

3.2.2.1. Variography: How does the spatial structure of VPUE varies between seasons?

Important variations in the variogram models can be observed between each trimester both in terms of the value of the variogram and the spatial structure described with variations in the nugget effect and spherical range and sill (see Annex X for the models' characteristics). No spatial structure was detected for the autumn (T4) for nets.

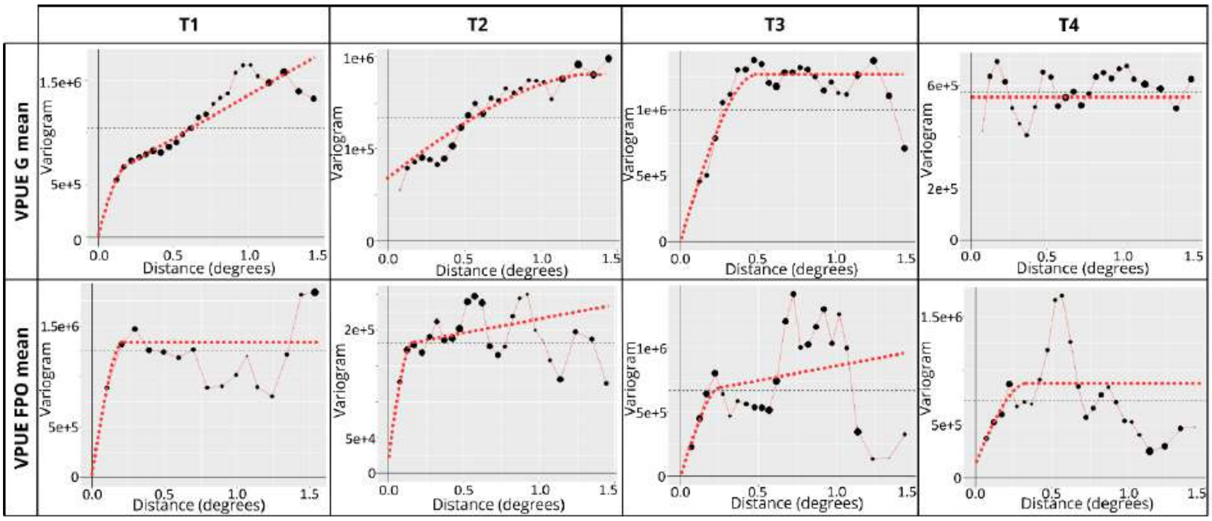

Figure 13: Experimental variograms (black dots with a diameter proportional to the number of pairs used in the calculation) and fitted model (red dotted line) used to produced kriging estimates of nets (G) and traps(FPO) VPUE, using averaged data ("mean"), for winter (T1), spring (T2), summer (T3) and autumn (T4). The black dotted line represents the variance of the data.

3.2.2.2. Maps of kriged VPUE: What seasonal variations can be observed for VPUE spatial distribution in the Gulf of Lion?

Important variation in both value and high VPUE localisation can be observed for nets (Figure 14) and traps (Figure 15) between trimesters.

The area with the highest VPUE for nets vary from an area centred around the OWF Gulf of Fos and Gulf of Lion East during the first two trimesters and an area more central next to the OWF Gulf of Lion Centre during the third trimester. The VPUE maximum values also vary during the year with the highest value for nets in winter and summer with respectively a maximum around 4000 and 5000 euros a day. The VPUE are lower in the spring with a maximum of 2000 euros a day. For traps the highest VPUE are estimated in winter, with around 7000 euros a day and the lowest in spring, with around 1750 euros a day.

These estimated spatial variations should be considered with caution as they us averaged data, and even more for the estimations for nets during autumn (T4) as the variogram model implies the use of a simple mean of values to estimate VPUE. The estimations for traps are also very uncertain in the OWF area as the value is extrapolated from observed data far from these areas.

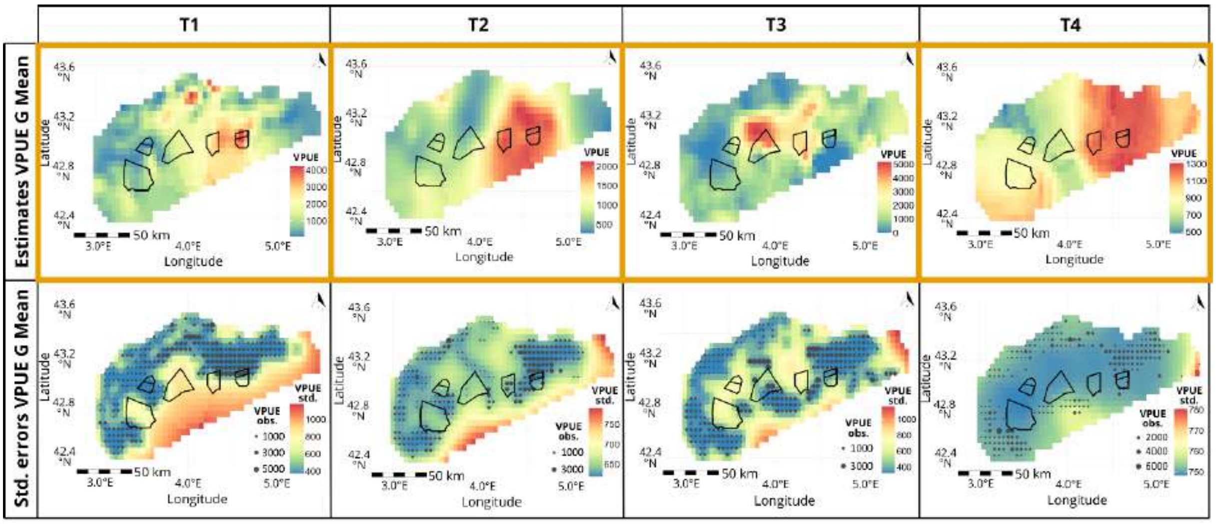

Figure 14: Maps of the VPUE (in euros/day) estimates and standard deviations (VPUE std.) in the Gulf of Lion obtained by kriging for nets (G) using averaged (mean) for winter (T1), spring (T2), summer (T3) and autumn (T4). The OWF areas are represented by a black contour and the observations by black dots (VPUE obs. in euros/day. The maps in orange should be used with cautions.

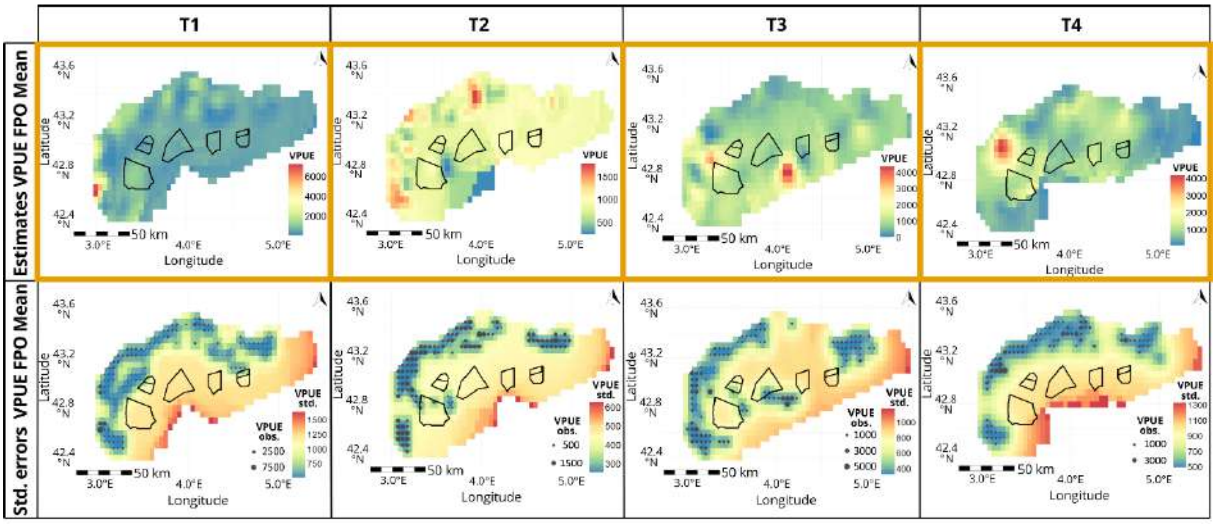

Figure 15: Maps of the VPUE (in euros/day) estimates and standard deviations (VPUE std.) in the Gulf of Lion obtained by kriging for traps (FPO) using averaged (mean) for winter (T1), spring (T2), summer (T3) and autumn (T4). The OWF areas are represented by a black contour and the observations by black dots (VPUE obs. in euros/day. The maps in orange should be used with cautions.

3.2.2.3. Predictions of VPUE in OWFs: Do VPUE estimates varies with the season?

For nets, the VPUE estimates fluctuate throughout the year for all the OWFs apart from the Gulf of lion West. The highest VPUE for the eastern most OWF (Gulf of Fos) are observed during winter (T1) with interval indicating a significant difference with the VPUE values in summer (T3), but not in spring (T2) for which we have larger confidence intervals. For the OWF closer to the centre of the Gulf of Lion (Narbonnaise, Gulf of Lion centre and Gulf of Lion East) the maximum VPUE are observed in summer (T3). The VPUE estimates are around 1000 euros a day for Narbonnaise which are not significantly different from the other seasons. For the other two OWFs the VPUE are around 3000 euros a day with no significant differences for the Gulf of Lion East, and significant differences with the second trimester for the Gulf of Lion Centre.

For traps, the VPUE estimates in the OWF areas (Table 6) are similar all year round. However, the confidence intervals are very large and include all values from zero to more than two thousand euros a day, except for the second trimester estimates whose confidence interval begin around 200 euros a day but stay relatively large.

Table 6 : VPUE estimates in each of the future OWF areas for nets (G) and traps (FPO) for winter (T1), spring (T2), summer (T3) and autumn (T4). The different OWFs are described by their abbreviation. Confidence intervals at 95 % are in brackets. All the estimations should be considered with caution.

	AO6N	AO6G	AO9N	AO9G	AO10	A10ans	A2050
VPUE G mean							
T1	**746,5** (0 – 2074)	**2455,8** (1142 – 3770)	**706,7** (0 – 1934)	**2402,4** (1092 – 3713)	**1471,3** (405 – 2537)	**2374,6** (1150 – 3599)	**819,2** (0 – 1717)
T2	**847,6** (0 – 2402)	**918,7** (0 – 2469)	**850,2** (0 – 2393)	**917,9** (0 – 2462)	**836,5** (0 – 2326)	**926,2** (0 – 2450)	**857,3** (0 – 2350)
T3	**1582,5** (463 – 2702)	**616,9** (306 – 928)	**1057,2** (5 – 2109)	**270,5** (0 – 79)	**2810,8** (2516 – 3106)	**3300,1** (2348 – 4252)	**613** (0 - 1267)
T4	NA	NA	NA	NA	NA	NA	NA
VPUE FPO mean							
T1	**688,2** (0 – 2207)	**794** (0 – 1940)	**589,4** (0 – 2084)	**849,5** (0 – 2467)	**909,5** (0 – 2239)	**900,6** (0 – 2542)	**843,3** (0 – 2066)
T2	**825,8** (167 – 1484)	**891,3** (228 – 1555)	**824,3** (232 – 1416)	**887,9** (254 – 1522)	**836** (393 – 1279)	**872,1** (304 – 1440)	**848,5** (450 – 1247)
T3	**1009,4** (0 – 2490)	**878,3** (0 – 2372)	**1066,3** (0 – 2462)	**907,8** (0 – 2369)	**1013,3** (0 – 2152)	**966,7** (0 – 2337)	**1179,6** (101 – 2258)
T4	**680,5** (0 – 2229)	**981,6** (0 – 2503)	**900,8** (0 – 2424)	**847,7** (0 – 2368)	**803,6** (0 – 2102)	**863,7** (0 – 2324)	**786** (0 – 2011)

3.2.2.4. Cross-validation

Table 7: Cross-validation statistics for the VPUE estimation by season through ordinary kriging (OK), using averaged data ("mean"), for nets (G) and traps (FPO) and from winter (T1) to autumn (T4)

Model	Mean prediction error	Mean squared prediction error	Mean standardized error
OK G VPUE mean T1	4.44	329093	1.33
OK G VPUE mean T2	2.23	330063	0.82
OK G VPUE mean T3	6.19	343715	1.61
OK G VPUE mean T4	16.16	536178	0.95
OK FPO VPUE mean T1	-12.93	972482	1.91
OK FPO VPUE mean T2	1.00	151980	1.41
OK FPO VPUE mean T3	-22.02	409320	1.48
OK FPO VPUE mean T4	11.46	292735	0.89

The cross-validation statistics are presented in Table 8. The mean prediction error is higher than the ones for the entire year in particularly for the estimation for fourth trimester for nets (G), which did not present a spatial structure and all trimesters, apart for the second one, for traps (FPO). The mean standardized errors are all close to 1 and do not indicate an important deviation from the expected value. In conclusion seasonal variations in the spatial structure for both nets and traps were detected. This variability is also present in terms of changes in VPUE values in OWFs for nets. However, these results should be used with caution due to the use of averaged data and the strong bias detected in most models.

4. Discussion

This prospective study aims to provide estimates of potential landings in weight and value in the future OWFs of the Gulf of Lion, if traps and nets are to be used in those zones. This report presents short-term LPUE estimates for four gear-species combinations: net-monkfish, net-hake, net-sole, and trap-octopus, and VPUE estimates for nets and traps. Several models were tested to produce these estimates. These models are characterized by increasing complexity, which is supposed to enhance the predictability and accuracy of the models.

4.1. Models' comparison and selection: Which model should be used ?

For each gear-species combination, we fitted four different models to estimates landings per unit of effort (LPUE in kg/day), two using only the gear-species observations (by kriging) and two using covariables (by cokriging). The covariables were the LPUE of other species caught by the same gear for the first one and the LPUE of the same species caught by trawl for the other. For each gear (traps and nets), four models were explored to produce value per unit of effort (VPUE in euros/day) estimates, the last two for accounting seasonal variations.

The differences between the two types of kriging model lies in the type of data used, either averaged or scattered. Using scattered data would be preferable as previously described. It accounts for all the variability in the observations and contrary to averaged data do not mix within the same random field model, data whose variance level is longer homogeneous (variance decreases by 1/number of averaged points), which violate the assumption of second order stationarity. Therefore, even if the models using scattered data perform less well when estimating LPUE, the use of this models will be prioritised. It isn't an issue for VPUE estimation as the models using scattered data performed better and therefore are selected.

The cokriging models aimed at improving LPUE predictions including covariables that are supposed to covariate spatially with the modelled LPUE and eventually that cover a wider area than the modelled LPUE. Two different covariables (tested in two different models) were considered to account for two different reasons of spatial covariance. The model using the LPUE observations of other species as covariable aimed at describing the mixed dimension of catches when using traps or nets However, the observations for the different variables used in cokriging must be collocated (Petitgas et al., 2017), which can be very restrictive when considering many species simultaneously. Depending on the data available, estimation for the entire study area is sometimes not feasible (Annex XI). Therefore, the use of this type of model is not optimal for making estimates and its results was not detailed in this report. The other model, using LPUE of same species by trawl as covariable, aimed at taking benefit of a wider spread observations of the same species and match with a more traditional application of cokriging. Indeed, as trawling data was reported at almost every square33 of the study area, it provides additional information in areas where the variable of interest was not observed directly (Petitgas et al., 2009 ; Petitgas et al., 2017). Looking at LPUE estimated by the univariate models using the same data configuration for each gear-species combination, the cokriging models produced estimates similar to those of ordinary kriging, with no significant differences in the LPUE estimates for each OWF. The quality of the fit (i.e. performance of the model), however, varies by species. For net-sole, the performance of the cokriging model was equivalent than the one of the kriging models, offering an interesting alternative. In contrast, the cokriging models for other gear-species combinations showed slightly worst performances. For instance, LPUE for trap-octopus, cokriging models showed respectively a poorer fit to the data according to the cross-validation and an unsatisfactory fit of the cross-variogram models.

Therefore, the use of cokriging model shows potential but it should be tested with other variables and using scattered data, which was not possible due to computation and time limitations. The models retained are thus the ones using scattered data. However, the LPUE estimates in OWFs for trap-octopus should be considered with caution as they were extrapolated from data which are closer to the coast. The models using averaged data should be considered with caution for the reasons detailed.

4.2. Nets and traps LPUE and VPUE estimations in the future OWFs' areas in the Gulf of Lion

4.2.1. Consistency between LPUE maps estimates and known species spatial distribution

In this study, we predicted potential LPUE across all future OWFs in the Gulf of Lion for four gear-species combinations : net-monkfish, net-hake, net-sole, and trap-octopus. For all species caught by nets, the predicted LPUE varies between OWFs.

The estimated LPUE for monkfish are quite low, averaging less than 40 kilograms per day across all OWFs. Note that these results do seem to align with the species' distribution as described in the literature, which indicates an even presence of the species on the continental shelf (Morfin et al., 2012 ; Vaz et al., 2023).

For hake, the selected model shows significantly higher LPUE values in the eastern part of the Gulf, which covers the OWFs Gulf of Fos and to a lesser extent the Gulf of Lion East. LPUE are estimated at around 250 and 110 kilograms per day in these areas, compared to 50 to 80 kilograms per day in other OWFs sites. These findings align with the estimated distribution of abundance of this species described in Morfin et al., (2012) study. While Vaz et al., (2023) suggest a slightly more homogenous distribution across the entire plateau, their study does not conflict with our estimates.

For sole, the area of high LPUE overlaps with the same two OWFs as hake, with LPUE estimates ranging from 100 to 110 kilograms per day. The estimated LPUE in other areas is slightly lower, at 20-70 kilograms per day. The high LPUE of sole in the eastern part of the Gulf could be linked to the positive influence of the Rhône plume on sole abundance, particularly in winter (the reference period used for this species in this study), when river discharges are higher (Gaertner et al. 1999 ; Salen Picard et al., 2002).

Finally, the LPUE estimates for octopus fished by traps were similar across all parks, ranging from 95 to 160 kilograms per day. The estimated average landings were slightly higher in the three OWFs in the centre and east of the gulf, though not significantly so compared to the other OWFs. The areas of high LPUE identified by our analysis along the coast correspond to areas of high common octopus (*Octopus vulgaris*) abundance (Vaz et al., 2023).

4.2.2. VPUE spatial distribution and its relationship with the LPUE for nets and traps

For nets, the areas with the highest estimated VPUE values are found in the eastern part of the gulf including the OWFs in the area: Gulf of Fos, Gulf of Lion East, and Gulf of Lion Centre. These estimates are consistent with the LPUE distribution for the three species fished by nets that are considered in this study. The estimates of VPUE in these OWFs are between €700 to €1000 per day with a confidence interval range around €1000/day. In the other OWFs, the VPUE is estimated around €400-500 with confidence intervals in the same range, that includes zero values for the OWF Narbonnaise.

For traps, the model used to estimate the income generated indicates that all the OWFs have a comparable potential income around €1100 per day. However, the confidence intervals are very large and sometimes include the possibility of zero income. As for LPUE maps estimates, the VPUE spatial distribution matches with those of octopus abundance s reported by Morfin et al. (2012) et Vaz et al. (2023), except for the area with high VPUE further offshore.

4.2.3. Seasonal variability of VPUE for nets and traps

Our results revealed potential seasonal variations in VPUE for both types of fishing gear considered, i.e. nets and traps. However, as explained previously these results should be considered with caution.

For nets fishing, seasonal differences in spatial patterns and in values of predicted VPUE were highlighted. The seasons of maximum VPUE varies depending on the OWF. In the easternmost OWF, the Gulf of Fos, the estimated maximum income is in winter and is significantly higher than in summer. The other OWF, except for the westernmost one, have maximum VPUE estimated in summer. For the two OWFs, Gulf of Lion Centre and Gulf of Lion East, the averaged estimated VPUE in winter is higher than in spring, unlike in the OWF Narbonnaise. These changes in potential revenue over the course of the year may reflect species seasonal migration. In particular, sole migrates offshore during the winter (Salen Picard et al., (2002)) and, according to our estimates, is caught more heavily in the eastern and central areas of the gulf. This is consistent with the high VPUE values estimated in the three corresponding OWFs. High VPUE values in summer correspond to periods of high monkfish and hake abundance related to recruitment in the OWFs areas (Vaz et al., 2023). The seasonal variations could also be linked to price variations depending on supply and demand.

For traps, according to the estimates, the spatial distribution of VPUE changes over the seasons, with areas of higher catches located closer to the coast from October to June, and further from the coast in summer. However, no significant change in potential income within the OWF areas could be detected. The average estimates remain consistent between seasons, albeit with wide confidence intervals. There are similarities between the areas of high abundance of horned octopus according to Vaz et al., (2023) and our estimates of high VPUE in the autumn and summer. Winter and spring may involve the fishing of more coastal species such as the common octopus (Vaz et al., 2023).

4.3. Limitations

This study was conducted using a novel combination of two spatial dishing data sources. The first one is derived from the Ifremer's SIH (based on reglementary data and SACROIS algorithm), which has been used in numerous previous studies leveraging this spatial information. The second source is the SATHOAN information system HALIOP, which has not yet been used in a study. Together, these sources provide complementary information on fishing in the Gulf of Lion, tracking the activity of different vessels – particularly thanks to HALIOP for vessels under 12 meters engaged in artisanal fishing (Guyader et al., 2013) – enabling us to make our estimates. However, the method used has its limitations and room for improvement remains.

4.3.1. A potentially biased estimate by using data unrepresentative of fishing activity

Even when these two sources of information are combined, the data used for our estimates only takes into account a fraction of the Mediterranean fleet that uses the fishing gears considered in the context of colocation. In fact, we only have information on average on 1.3% of vessels using nets and 10% on average on the ones using traps. Therefore, the information used in our study may not be representative of the fleet's activity, which could introduce bias into our estimates, particularly those of net fishing.

4.3.2. Uncertainty in the input tidy data for predicting LPUE and VPUE in OWFs

In addition to the limitations imposed by the raw data, the method used to prepare the data on which we adjusted the models has its own limitations. The harmonisation of the two data sources is imperfect. Differences remain in the calculation of effort and the spatial distribution of catches (Figure 6). These differences may introduce bias into our estimates. Additionally, the chosen scale of effort causes us to lose accuracy in the SACROIS data. This scale, which has not been applied to trawler data, also potentially reduces the correlation between landings from the two fishing gears for a given species, thus affecting the cokriging predictions. Further work on effort distribution could improve the models.

The standardisation of data used for LPUE and VPUE of nets and traps also has limitations. Potential differences between vessels could not be taken into account in the standardisation due to the collinearity between the vessel effect and the spatial effect. We can therefore assume that some of the variability due to the vessel has not been compensated for. However, the quality of the standardisation model is important because it significantly alters the LPUE and VPUE values (see Annex IX for the comparison). The use of standardisation to get rid of the temporal variations in the data is also less optimal than producing one map per year or per month More in-depth work on this preliminary standardisation of data would be beneficial to improving the model.

4.4. Key findings including limitations

Due to the limitations mentioned above, predictions of catches and revenues in the parks should be treated with caution. However, our study enabled us to estimate the VPUE in the OWFs, accompanied by a confidence interval for nets and traps. Furthermore, for nets, a link was found between the estimated spatial distribution of VPUE and that of LPUE for the three species of high economic interest detailed in this study. Seasonal variability in VPUE was also observed for this gear type. The three easternmost wind farms offer significant landing opportunities in terms of weight and value, especially for net fishing, according to the landing profile for the three studies species. However, the two westernmost OWFs offer fewer opportunities. A following study on the profitability of a colocation activity, potentially a seasonal one would bring a more global vision on the implementation of colocation between OWFs and fisheries.

The use of cokriging to improve model prediction showed potential particularly for the LPUE estimation of net-sole and net-monkfish with clear spatial covariance between the variables considered. Further exploration around this method could allow an improvement of model predictions.

4.5. Perspectives

4.5.1. Using data with a finer spatial scale to describe spatial structure at short distances

The SACROIS data we used were aggregated by square33. However, this fishing data is available on request in a non-aggregated format, with precise GPS positions transmitted by VMS. Using this data in conjunction with HALIOP data would enable us to render the spatial structure at short distances, which is not possible in this study.

4.5.2. Cokriging models improvement through additional covariables

Additional covariables could be incorporated into the current cokriging models exploiting trawler fishing data. The use of environmental variables was considered but not implemented by lack of time. Variables such as the bathymetry, sediment type or bottom temperature could be correlated with the LPUE of different species and therefore provide additional information if they are included in the model (Petitgas et al., 2017). These data could enable the models to account for the influence of habitat on the abundance or catchability of species in different areas. Using species abundance indices as covariables could also be explored. For example, indices based on data from the MEDITS scientific campaigns in the Mediterranean could provide information on species spatial distribution. Finally, another source of information could provide data on the unobserved part of the fleet in our study. The Ifremer's SIH collects data on the entire fleet, but only the fishing activity associated to a VMS signal are spatialised. However, trials are being conducted to spatialise the catches reported on logbooks by cross-referencing this fishing data with the fishers' declarations on activity calendars, which specifies the area where fishing occurred. This would provide spatially referenced information on the entire fleet, albeit on a coarser spatial scale than for the data used in this study.

4.5.3. Improving models by considering the potential anisotropy of the spatial structure

Both ordinary kriging models and cokriging models fitted are based on variogram models assuming isotropy. However, the presence of a gradient from the coast to the open sea, characterised for example by the bathymetry gradient influences the abundance of many species, for example sole (Gaertner et al. (1999)). The variability along the gradient we increase more rapidly than along the isobath which are perpendicular to the gradient. This results in an anisotropy that should be considered in the variogram models. This is done by calculating experimental variogram and fitting a model for different directions, for example two orthogonal directions (Petitgas et al., 2017).

4.5.4. Towards medium- to long-term predictions to compare management scenarios

This study provides preliminary estimates of the potential landings (in weight) by species and revenues by gear from the colocation between OWFs and commercial fishing activity. It provides an initial overview of the short-term potential of this new activity, using fishing gears, as far as we are aware, that are rarely used in those areas by a handful of vessels.

However, this does not provide an overview of these potential landings and their evolution on a medium- or long-term period. Indeed, the construction of OWFs combined with the installation of artificial reefs as part of the Fishwind project could greatly alter the ecosystem in proximity to these new hard structures (Agdé et al., 2024; Lloret et al., 2025; van Hoey et al., 2021; Watson et al., 2024). The floats of the wind turbines and other structures in the water column could attract pelagic species in the same way as FADs (Fish Aggregating Device) (Fayram & de Risi, 2007; Wilhelmsson et al., 2006). Reef shelters and wind turbine anchors can attract new species, such as crustaceans, which seek this type of hard substrates with cavities. This has been observed for crustaceans (Rozemeijer et al., 2024; Stelzenmüller et al., 2021), as well as for demersal fishes such as cod or pouting (Reubens et al., 2013) in the North Sea. Fisheries targeting these species within and around wind farms have been considered (Adgé et al., 2024; Rozemeijer et al., 2024; Stelzenmüller et al., 2021). Depending on the shape and complexity of the chosen artificial reefs, it is expected that species of interest to fisheries will be attracted and their biomass increased (Langhamer, 2012; Layman & Allgeier, 2020; Pondella at al., 2022), to support sustainable fishing in these areas (OP SATHOAN, 2025).

To make medium- to long-term predictions of landings in weight and value, and to test different management scenarios, this preliminary study could be followed up with the use of fishery dynamics models. Using the ISIS-Fish model (Mahévas & Pelletier, 2004), for example, would enable us to model the fishery evolution and behaviour under different management scenarios, and therefore assess the impact of implementing colocation versus closing OWF areas entirely.

References

Bibliography

Adgé, M., Lobry, J., Tessier, A., & Planes, S. (2024). Modeling the impact of floating offshore wind turbines on marine food webs in the Gulf of Lion, France. *Frontiers in Marine Science*, *11*, 20. [online], viewed on 24/08/2025 https://doi.org/10.3389/fmars.2024.1379331

Aidoo, E. N., Mueller, U., Goovaerts, P., & Hyndes, G. A. (2015). Evaluation of geostatistical estimators and their applicability to characterise the spatial patterns of recreational fishing catch rates. *Fisheries Research*, *168*, 20-32. [online], viewed on 14/08/2025 https://doi.org/10.1016/j.fishres.2015.03.013

Alexander, K. A., Potts, T., & Wilding, T. A. (2013). Marine renewable energy and Scottish west coast fishers : Exploring impacts, opportunities and potential mitigation. *Ocean & Coastal Management*, *75*, 1-10. [online] , viewed on 06/03/2025 https://doi.org/10.1016/j.ocecoaman.2013.01.005

Arrêté du 10 janvier 2012 fixant les règles d'emport et d'utilisation des équipements d'enregistrement et de communication électroniques des données relatives aux activités de pêche à bord des navires sous pavillon français ainsi que des navires sous pavillon étranger qui se trouvent dans les eaux sous juridiction française, Pub. L. No. NOR : AGRM1131385A, A. (2012). [online] , viewed on 10/08/2025 https://www.legifrance.gouv.fr/loda/id/JORFTEXT000025193618

Bonsu, P. O., Letschert, J., Yates, K. L., Svendsen, J. C., Berkenhagen, J., Rozemeijer, M. J. C., Kerkhove, T. R. H., Rehren, J., & Stelzenmüller, V. (2024). Co-location of fisheries and offshore wind farms : Current practices and enabling conditions in the North Sea. *Marine Policy*, *159*, 11. [online] , viewed on 05/03/2025 https://doi.org/10.1016/j.marpol.2023.105941

Campbell, M., Samhouri, J. F., & White, J. W. (2025). Modeling consequences of spatial closures for offshore energy : Loss of fishing grounds and fishery-independent data. *Ecosphere*, *16*(7), 15. [online] , viewed on 06/08/2025 https://doi.org/10.1002/ecs2.70336

Cressie, N. (1985). Fitting variogram models by weighted least squares. *Journal of the International Association for Mathematical Geology*, *17*(5), 563-586. [online] , viewed on 14/08/2025 https://doi.org/10.1007/BF01032109

de Groot, J., Campbell, M., Ashley, M., & Rodwell, L. (2014). Investigating the co-existence of fisheries and offshore renewable energy in the UK : Identification of a mitigation agenda for fishing effort displacement. *Ocean & Coastal Management*, *102*, 7-18. [online] , viewed on 06/03/2025 https://doi.org/10.1016/j.ocecoaman.2014.08.013

Dunkley, F., & Solandt, J.-L. (2022). Windfarms, fishing and benthic recovery : Overlaps, risks and opportunities. *Marine Policy*, *145*, 8. [online] , viewed on 06/08/2025 https://doi.org/10.1016/j.marpol.2022.105262

Dupont, C., Herpers, F., & Le visage Christophe. (2020). *Recommendations for positive interactions between offshore wind farms and fisheries : Short background study* (e-ISBN 978-92-9460-158-2; p. 26). European Commission. [online] , viewed on 14/08/2025 https://strategies-marines.fr/wp-content/uploads/2022/05/recommendations_for_positive_interactions_between_offshore_wind_farms_and_fisheries.pdf.pdf

Farrugio, H., & Le Corre, G. (1986). *Interactions entre pêcheries de lagunes, pêcheries côtières et pêche au chalut dans le golfe du Lion* (DRV-86.003/RH; p. 213). Ifremer. [online] , viewed on 23/08/2025 https://archimer.ifremer.fr/doc/00000/1655/

Fayram, A. H., & de Risi, A. (2007). The potential compatibility of offshore wind power and fisheries : An example using bluefin tuna in the Adriatic Sea. *Ocean & Coastal Management*, *50*(8), 597-605. [online] , viewed on 18/03/2025 https://doi.org/10.1016/j.ocecoaman.2007.05.004

Gaertner, J. C., Mazouni, N., Sabatier, R., & Millet, B. (1999). Spatial structure and habitat associations of demersal assemblages in the Gulf of Lions : A multicompartmental approach. *Marine Biology*, *135*(1), 199-208. [online] , viewed on 06/08/2025 https://doi.org/10.1007/s002270050617

Gonzales, C. M., Chen, S., & Froehlich, H. E. (2024). Synthesis of multinational marine aquaculture and clean energy co-location. *Frontiers in Aquaculture*, *3*, 13. [online] , viewed on 26/07/2025 https://doi.org/10.3389/faquc.2024.1427839

Goovaerts, P. (1997). *Geostatistics for Natural Resources Evaluation*. Oxford University Press. [online] , viewed on 18/05/2025 https://books.google.fr/books?hl=fr&lr=&id=CW-7tHAaVR0C&oi=fnd&pg=PA3&dq=goovaerts+1997+krigeage&ots=zlthvU8MnD&sig=Vt27gTNbrmG05m-O9HeoskVeoMQ#v=onepage&q&f=false

Gray, T., Stromberg, P.-L., & Rodmell, D. (2016). *Changes to fishing practices around the UK as a result of the development of offshore windfarms – Phase I (Revised)* (p. 121). The Crown Estate. [online] , viewed on 16/03/2025 https://www.thecrownestate.co.uk/media/2600/final-published-ow-fishing-revised-aug-2016-clean.pdf

Guşatu, L. F., Zuidema, C., & Faaij, A. (2022). A multi-criteria analysis framework for conflict resolution in the case of offshore wind farm sitting : A study of England and the Netherlands offshore space. *Frontiers in Marine Science*, *9*, 29. [online] , viewed on 10/08/2025 https://doi.org/10.3389/fmars.2022.959375

Guyader, O., Berthou, P., Koutsikopoulos, C., Alban, F., Demanèche, S., Gaspar, M. B., Eschbaum, R., Fahy, E., Tully, O., Reynal, L., Curtil, O., Frangoudes, K., & Maynou, F. (2013). Small scale fisheries in Europe : A comparative analysis based on a selection of case studies. *Fisheries Research*, *140*, 1-13. [online] , viewed on 24/08/2025 https://doi.org/10.1016/j.fishres.2012.11.008

Hooper, T., & Austen, M. (2014). The co-location of offshore windfarms and decapod fisheries in the UK : Constraints and opportunities. *Marine Policy*, *43*, 295-300. [online] , viewed on 14/03/2025 https://doi.org/10.1016/j.marpol.2013.06.011

Ifremer. (2022). *Sacrois. Un algorithme de croisement de données*. Archimer. [online] , viewed on 21/08/2025 https://archimer.ifremer.fr/doc/00774/88631/

Ifremer. (2024a). *Flotte de la façade Méditerranée. 2023. Synthèse des flottilles de pêche.* (102505; Système d'Information Halieutiques, p. 14). Ifremer. [online] , viewed on 18/07/2025 https://archimer.ifremer.fr/doc/00913/102505/

Ifremer, S. (2024b). *Algorithme de traitement de données de géolocalisation ALGOPESCA* (Note Synthétique 79405; p. 27). Ifremer. [online] , viewed on 12/06/2025 https://archimer.ifremer.fr/doc/00682/79405/

Jadaud, A., Mellon, C., Berthou, P., & Biseau, A. (2015). *Interactions spatiales et temporelles entre effort de pêche et répartition des biomasses de rouget et merlu dans le golfe du Lion* (Réponse à la saisine DPMA N°15-8503 41031; p. 32). Ifremer. [online] , viewed on 24/05/2025 https://archimer.ifremer.fr/doc/00299/41031/

Langhamer, O. (2012). Artificial Reef Effect in relation to Offshore Renewable Energy Conversion : State of the Art. *The Scientific World Journal*, *2012*(1), 386713. [online] , viewed on 23/08/2025 https://doi.org/10.1100/2012/386713

Layman, C. A., & Allgeier, J. E. (2020). An ecosystem ecology perspective on artificial reef production. *Journal of Applied Ecology*, *57*(11), 2139-2148. [online] , viewed on 23/08/2025 https://doi.org/10.1111/1365-2664.13748

Lloret, J., Wawrzynkowski, P., Dominguez-Carrió, C., Sardá, R., Molins, C., Gili, J. M., Sabatés, A., Vila-Subirós, J., Garcia, L., Solé, J., Berdalet, E., Turiel, A., & Olivares, A. (2025). Floating offshore wind farms in Mediterranean marine protected areas : A cautionary tale. *ICES Journal of Marine Science, fsad131*, *82*(3), 14. [online] , viewed on 24/08/2025 https://doi.org/10.1093/icesjms/fsad131

Macron, E. (2022). *Déclaration de M. Emmanuel Macron, président de la République, sur la politique de l'énergie, à Belfort le 10 février 2022*. [online] , viewed on 28/03/2025 https://www.vie-publique.fr/discours/283773-emmanuel-macron-10022022-politique-de-lenergie

Mahévas, S., & Pelletier, D. (2004). ISIS-Fish, a generic and spatially explicit simulation tool for evaluating the impact of management measures on fisheries dynamics. *Ecological Modelling*, *171*(1), 65-84. [online] , viewed on 22/08/2025 https://doi.org/10.1016/j.ecolmodel.2003.04.001

Mignucci, A. (2021). *Rôle de l'environnement dans la dynamique spatiale des poissons marins à l'interface lagune-mer en Méditerranée française : Approches d'écologie spatiale et d'écophysiologie appliquées à trois espèces côtières* [Phdthesis, Université Montpellier]. [online] , viewed on 23/08/2025 https://theses.hal.science/tel-03615101

Ministère de la transition écologique et solidaire. (2019). *Programmation pluriannuelle de l'énergie 2019-2028* (Stratégie française pour l'énergie et le climat, p. 400). [online] , viewed on 12/05/2025 https://www.ecologie.gouv.fr/politiques-publiques/programmations-pluriannuelles-lenergie-ppe

Ministère de la transition écologique et solidaire. (2020). *Stratégie nationale bas-carbone : La transition écologique et solidaire vers la neutralité carbone* (p. 192). [online] , viewed on 12/05/2025 https://www.ecologie.gouv.fr/politiques-publiques/strategie-nationale-bas-carbone-snbc

Morfin, M., Bez, N., & Fromentin, J.-M. (2016). Habitats of ten demersal species in the Gulf of Lions and potential implications for spatial management. *Marine Ecology Progress Series*, *547*, 219-232. [online] , viewed on 12/08/2025 https://doi.org/10.3354/meps11603

Morfin, M., Fromentin, J.-M., Jadaud, A., & Bez, N. (2012). Spatio-Temporal Patterns of Key Exploited Marine Species in the Northwestern Mediterranean Sea. *PLoS ONE*, *7*(5), 14, e37907. [online] , viewed on 12/08/2025 https://doi.org/10.1371/journal.pone.0037907

Oliver, M. A., & Webster, R. (2014). A tutorial guide to geostatistics : Computing and modelling variograms and kriging. *CATENA*, *113*, 56-69. [online] , viewed on 22/07/2025 https://doi.org/10.1016/j.catena.2013.09.006

Petitgas, P. (2009). Geostatistics and Their Applications to Fisheries Survey Data : A History of Ideas, 1990–2007. In B. A. Megrey & E. Moksness (Éds.), *Computers in Fisheries Research* (2e éd., p. 191-224). Springer Netherlands. [online] , viewed on 15/07/2025 https://doi.org/10.1007/978-1-4020-8636-6_7

Petitgas, P., Poulard, J. C., & Biseau, A. (2003). Comparing commercial and research survey catch per unit of effort : Megrim in the Celtic Sea. *ICES Journal of Marine Science*, *60*(1), 66-76. [online] , viewed on 08/06/2025 https://doi.org/10.1006/jmsc.2002.1321

Petitgas, P., Woillez, M., Rivoirard, J., Renard, D., & Bez, N. (2017). Handbook of Geostatistics in R for Fisheries and Marine Ecology. *ICES WGACEGG*, *338*, 184. [online], viewed on 20/08/2025 https://doi.org/10.17895/ices.pub.3717

Pondella, D. J., Claisse, J. T., & Williams, C. M. (2022). Theory, practice, and design criteria for utilizing artificial reefs to increase production of marine fishes. *Frontiers in Marine Science*, *9*, 14. [online] , viewed on 25/08/2025 https://doi.org/10.3389/fmars.2022.983253

RÈGLEMENT (UE) 2019/ 1022 DU PARLEMENT EUROPÉEN ET DU CONSEIL - du 20 juin 2019 - établissant un plan pluriannuel pour les pêcheries exploitant des stocks démersaux en Méditerranée occidentale et modifiant le règlement (UE) n° 508/2014, Pub. L. No. 2019/1022, 17 (2019).

Reubens, J. T., Braeckman, U., Vanaverbeke, J., Van Colen, C., Degraer, S., & Vincx, M. (2013). Aggregation at windmill artificial reefs : CPUE of Atlantic cod (*Gadus morhua*) and pouting (*Trisopterus luscus*) at different habitats in the Belgian part of the North Sea. *Fisheries Research*, *139*, 28-34. [online] , viewed on 24/08/2025 https://doi.org/10.1016/j.fishres.2012.10.011

Roach, M., Cohen, M., Forster, R., Revill, A. S., & Johnson, M. (2018). The effects of temporary exclusion of activity due to wind farm construction on a lobster (Homarus gammarus) fishery suggests a potential management approach. *ICES Journal of Marine Science*, *75*(4), 1416-1426. [online] , viewed on 06/03/2025 https://doi.org/10.1093/icesjms/fsy006

Rozemeijer, M. J. C., Deetman, B., Baan, C., Cramer, R., Leemans, E., Korving, A., Pronk, R., & Taal, K. (2024). *Win-Wind eindrapport : De eerste stap in het concreet vormgeven van passieve visserij op Noordzeekrab en Europese kreeft als een vorm van medegebruik* (C007/24; Wageningen Marine Research rapport, p. 34). Wageningen Marine Research. [online] , viewed on 10/03/2025 https://research.wur.nl/en/publications/win-wind-eindrapport-de-eerste-stap-in-het-concreet-vormgeven-van

Salen-Picard, C., Darnaude, A. M., Arlhac, D., & Harmelin-Vivien, M. L. (2002). Fluctuations of macrobenthic populations : A link between climate-driven river run-off and sole fishery yields in the Gulf of Lions. *Oecologia*, *133*(3), 380-388. [online] , viewed on 23/08/2025 https://doi.org/10.1007/s00442-002-1032-3

Sans, M., & Rodriguez, J. (2023). Développement et application d'une chaîne de traitement combinant apprentissage statistique et géo-informatique pour évaluer l'effort engin des fileyeurs opérant dans le Golfe de Gascogne. *Ifremer*, 52. archimer. [online] , viewed on 26/08/2025 https://doi.org/10.13155/97561

Stelzenmüller, V., Gimpel, A., Haslob, H., Letschert, J., Berkenhagen, J., & Brüning, S. (2021). Sustainable co-location solutions for offshore wind farms and fisheries need to account for socio-ecological trade-offs. *Science of The Total Environment*, *776*(145918), 12. [online] , viewed on 06/03/2025 https://doi.org/10.1016/j.scitotenv.2021.145918

Stockbridge, J., Brown, C. J., & Kuempel, C. D. (2025). Mapping the global co-location potential of offshore wind energy and aquaculture production. *Ocean & Coastal Management*, *263*(107605), 9. [online] , viewed on 07/08/2025 https://doi.org/10.1016/j.ocecoaman.2025.107605

Strietman, W. J., Deetman, B., Rozemeijer, M. J. C., & Kunz, M. C. (2023). *De commerciële haalbaarheid van passieve visserij op Noordzeekrab in windparken voor de Hollandse kust : Een verkenning naar de potentiële kosten en opbrengsten* (611467; p. 28). Wageningen Economic Research. [online] , viewed on 07/03/2025 https://library.wur.nl/WebQuery/wurpubs/611467

Szostek, C. L., Watson, S. C. L., Trifonova, N., Beaumont, N. J., & Scott, B. E. (2025). Spatial conflict in offshore wind farms : Challenges and solutions for the commercial fishing industry. *Energy Policy*, *200*(114555), 10. [online] , viewed on 06/08/2025 https://doi.org/10.1016/j.enpol.2025.114555

University MINES Paris-PSL. (2025). *gstlearn : The Geostatistics and Machine Learning C++ Library, Python and R Packages* (Version 1.8.0) [R]. Zenodo. https://doi.org/10.5281/zenodo.15865397

Van Hoey, G., Bastardie, F., Birchenough, S., De Backer, A., Gill, A., de Koning, S., Hodgson, S., Mangi Chai, S., Steenbergen, J., Termeer, E., van den Burg, S., & Hintzen, N. (2021). *Overview of the effects of offshore wind farms on fisheries and aquaculture* (Final Report EASME/EMFF/2018/011 Lot 1: Specific Contract No. 03; Publications Office of the European Union, p. 99). European Commission. [online] , viewed on 24/08/2025 https://cinea.ec.europa.eu/publications/digital-publications/overview-effects-offshore-wind-farms-fisheries-and-aquaculture_en

Vaz, S., Certain, G., Hattab, T., Jadaud, A., Villeneuve, R., Raphalen, E., Metral, L., Cheret, I., Bourdeix, J.-H., Tessier, E., Hattab, T., Jadaud, A., Villeneuve, R., Raphalen, E., Metral, L., Cheret, I., Bourdeix, J.-H., & Tessier, E. (2023). *Suivi spatio-temporel des espèces démersales et benthiques : Rapport final de l'action 3 du Projet GOLDYS* (96823; RBE/MARBEC/LHM 2023, p. 108). Ifremer. [online] , viewed on 14/08/2025 https://doi.org/10.13155/96823

Watson, S. C. L., Somerfield, P. J., Lemasson, A. J., Knights, A. M., Edwards-Jones, A., Nunes, J., Pascoe, C., McNeill, C. L., Schratzberger, M., Thompson, M. S. A., Couce, E., Szostek, C. L., Baxter, H., & Beaumont, N. J. (2024). The global impact of offshore wind farms on ecosystem services. *Ocean & Coastal Management*, *249*(107023), 11. [online], viewed on 24/08/2025 https://doi.org/10.1016/j.ocecoaman.2024.107023

Weiss, J., & Système d'Information Halieutique de l'Ifremer. (2020). *Détermination des seuils de vitesse de pêche par flottille* (rapport scientifique 77340; p. 60). Ifremer. [online], viewed on 21/07/2025 https://archimer.ifremer.fr/doc/00661/77340/

Wilhelmsson, D., Malm, T., & Öhman, M. C. (2006). The influence of offshore windpower on demersal fish. *ICES Journal of Marine Science*, *63*(5), 775-784. [online], viewed on 24/08/2025 https://doi.org/10.1016/j.icesjms.2006.02.001

Wright, K., Mair, J., Watret, R., & Drewery, J. (2023). *Static fishing gear trials at the Hywind floating offshore wind farm* (p. 66). Marine Directorate, Scottish Government. [online] , viewed on 19/03/2025 https://cdn.equinor.com/files/h61q9gi9/global/f4acf4706c8b0ab0a270a1950e12cefb38361b6c.pdf?hywind-static-fishing-gear-trial-report.pdf

Webograpphy

Ailes Marines. (2024). L'exploitation du parc éolien en mer. *Ailes Marines*. [online], viewed on 24/03/2025 https://ailes-marines.bzh/lexploitation-du-parc-eolien-en-mer/

Cerema. (2024). *Golfe du Lion Centre*. Eoliennes en mer en France. [online], viewed on 23/03/2025 https://www.eoliennesenmer.fr/facades-maritimes-en-france/facade-mediterranee/golfe-lion/centre

Cerema. (2025). *Façade Méditerranée*. Eoliennes en mer en France. [online], viewed on 23/03/2025 https://www.eoliennesenmer.fr/facades-maritimes-en-france/facade-mediterranee

CNDP. (2024, juillet 25). *La mer en débat : Environnement, éolien en mer, activités maritimes et littoral*. CNDP. [online] , viewed on 02/04/2025 https://www.debatpublic.fr/la-mer-en-debat

Eolenmer. (2023). Présentation. *Eolenmer Observatoire*. [online], viewed on 23/03/2025 https://recherche-eolenmer.fr/presentation/

Eolienne Offshore des Hautes Falaises. (2024). *La pêche professionnelle | Parc éolien en mer de Fécamp*. [online], viewed on 23/03/2025 https://parc-eolien-en-mer-de-fecamp.fr/suivi-chantier/la-peche-professionnelle/

France Energies Marines. (2025). *FISHOREMAN*. France Energies Marines. [online], viewed on 22/03/2025 https://www.france-energies-marines.org/projets/fishoreman/

OP SATHOAN. (2025a). *Fishwind coexistence pêche éolien biodiversité durable*. fishwind. [online], viewed on 24/06/2025 https://www.fishwind.fr/

OP SATHOAN. (2025b). *Réunion de lancement du projet Fishwind* [Réunion de projet].

Parc du Banc de Guérande. (2024). Navigation et sécurité maritime | Parc éolien en mer de Saint-Nazaire. *Parc éolien en mer de St-Naziare*. [online], viewed on 24/03/2025 https://parc-eolien-en-mer-de-saint-nazaire.fr/environnement/navigation-et-securite-maritime/

ANNEXES

Annex I: Phases and steps of the Fishwind project (OP SATHOAN, 2025a).

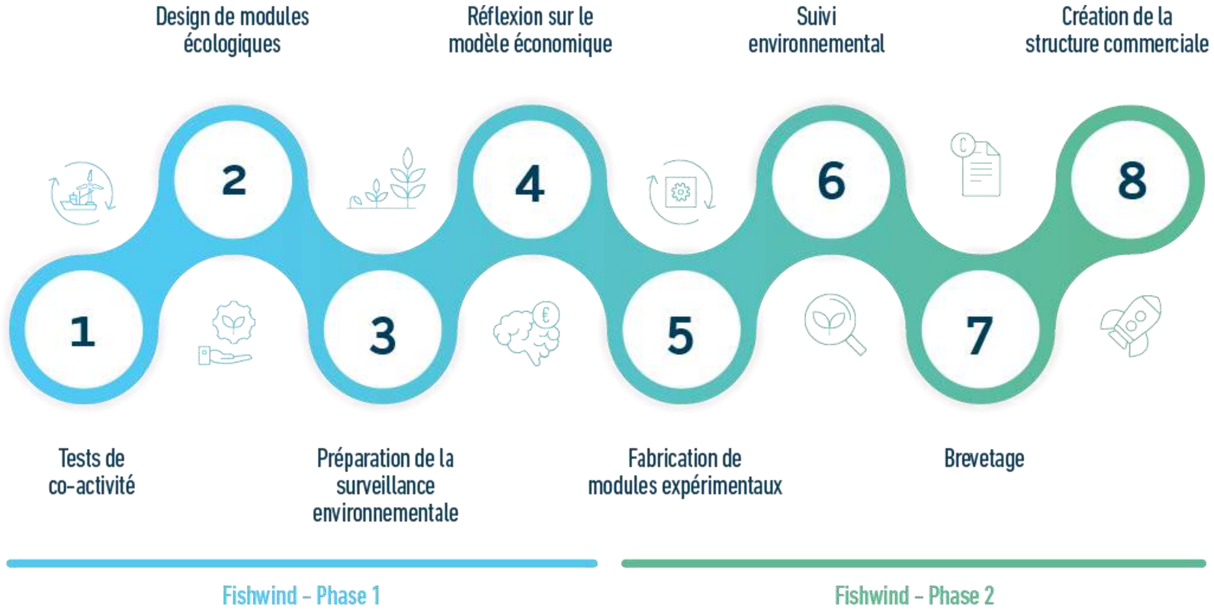

Annex II: A: Number of vessels that used at least one of the fishing gears concerned by the co-location between 2015 and 2024 in the datasets from HALIOP and SACROIS; B: Cumulative number of vessels that used at least one of the fishing gears concerned by the co-location between 2015 and 2024.

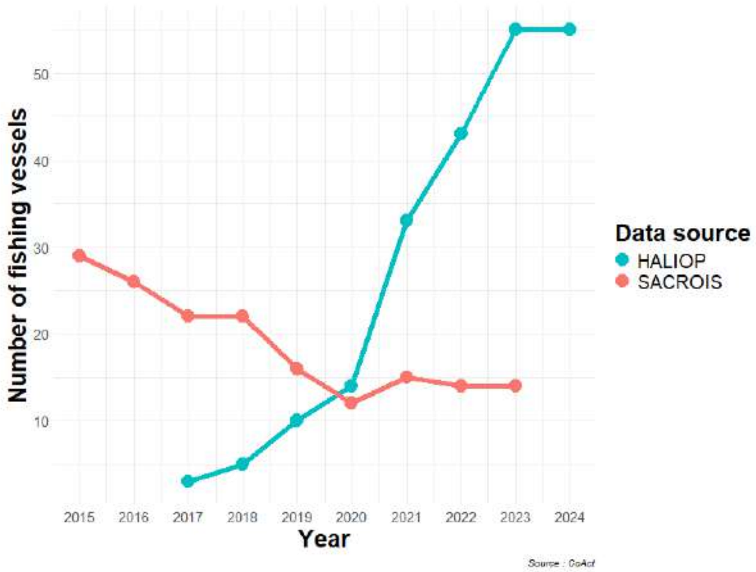

A

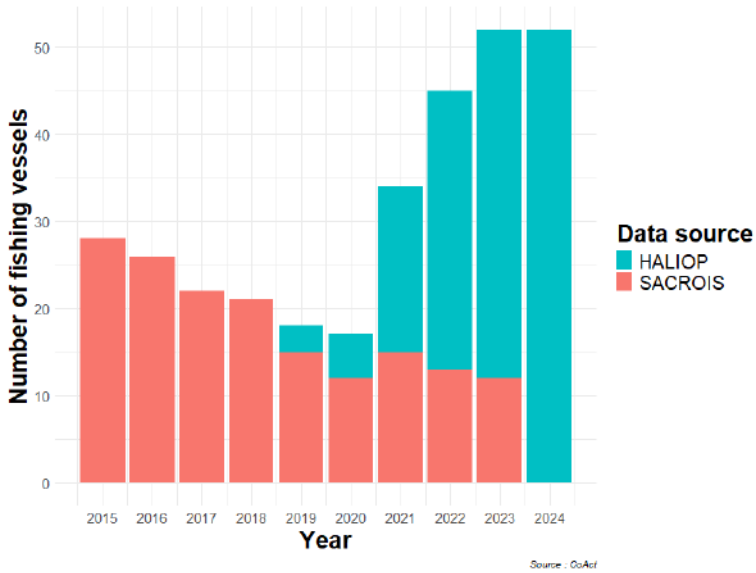

B

Annex III: FAO codes included in each fishing gear group

Fishing gear groups	Fishing gears considered in the group
OT	OTB, OTT, OTM, TM, PTM
G	GN, GNC, GND, GNF, GNS, GEN, GTN, GTR, LNS, LNP, LNB, LN
FPO	FPO, FYK
LL	LL, LLS, LLD
PS	PS, PS1, PS2, LA
LH	LHM, LHP, LTL, LX

Annex IV: FAO codes of the species attributed to each of the species groups

Groupe	Codes FAO	Groupe	Codes FAO
Acoupa	NBM, YNM	Daurade autre	SBP
Alose	ASD, SHD	Daurade grise	BRB
Anchois	ANE	Daurade rose	SBR
Anguille	ELE	Daurade royal	SBG
Araignée	SCR	Dente	DEC, SBX
Argentine	ARG, ARU, ARY	Donzelle	OOA, OSG, WRA
Anthéridies	SIL	Empereur	LHN, LTK
Auxide	FRI	Eperlan	SME
Bar	BSE, BSS	Espadon	SWO
Barbue	BLL	Feuille	CIL
Baudroie	ANG, MNZ, MON	Flet	FLE
Beauclaire	BIG	Gastéropodes autre	FMS, GAS, HLT, MOL, MOL, NSQ, PEE, WHE
Bécune	BAC, BAR, BAZ, GBA	Gobies	GOB
Bivalves autre	CLH, CLX, QSC, RAZ, SCE, SJA , SSP, TWL	Grenadier	RHG
Blennies	BLE	Grondin	CTZ, GUG, GUN, GUR, GUU, GUX
Bogue	BOG	Holoturie	CUX, JCR
Bonite	BON, BZX	Hoplostête	HPR, ORY
Brosme	USK	Huitre	OYC, OYF, OYG
Calmar	ILL, OUL, OUW, SQR, SQU, SQZ	Labre	YFX
Capelan	CAP, POD	Lamprois	LAG
Carangue	CXS	Langoustes et homards	LBE, LOX, LOY, PSL, SLO, VLO
Cardine	LEZ, MEG	Langoustine	NEP, NEX
Carpe	FCP	Liche	LEE, POP
Castagnole	POA	Lieu	POL
Centrolophe	CEO	Limande	DAB, FLW, LEF, LEM
Cépole	CBC	Maigre	MGR
Chimère	HYD	Makaire	BIL, BLM, BUM, MLS, MSP, WHM
Chinchard	HMM, HOM, JAX	Maquereau	MAC, MAS, MAX, VMA
Congre	COE	Marbre	SSB
Coques	COC, COZ	Merlan	WGH, WHG
Cordonnier	LTA	Merlan bleu	WHB
Coryphène	DOL, DOX	Merlu	HKE
Crabe	CMR, CRA, CRB, CRE, CRG, IOD, LIO	Mérou	GPD, GPX, WRF
Crevette	ARA, ARS, CPR, CSH, DCP, DPS, KUP, PEN, PNB, PRA, TGS	Morue	COD
Crustacés autre	CRU, CZM, PCB	Motelle	ROL

Sériole	AMB, YTL	Moule	MSM, MYV
Mulet	MGA, MGC, MGS, MLR, MUF, ODL	Serran	BAS, CBR
Murène	MMH	Silure	FSI, MGL
Murex	BOY, FNT	Sole	MKG, OAL, SOL, SOS, SOX
Non spécifié	MZZ, ZZ9	Sparaillon	ANN
Oblade	SBS	Sprat	SPR
Ombrine	UCA	Squille	OIL, SCY, SQY
Orphie	GAR	Tacaud	BIB
Oursin	URM, URX	Tassergal	BLU
Pageot	PAC, PAX, SBA	Thazard	KGX
Pagre	RPG	Thon	ALB, BET, SKJ, TUN, YFT
Petite sole	GSM	Thon rouge	BFT
Phycis	FOR, GFB	Turbot	TUR
Picarel	BPI, SPC	Uranoscope	UUC
Plie	PLE	Vieille	USB
Poisson lune	MOX	Violet	SSG
Poisson plat	FLX	Vive	WEG
Poisson ruban	TRX		
Poisson sabre	CUT		
Poulpe	EOI, OCC, OCM, OCT, OCZ		
Raie	JDP, JRS, MYL, RAJ, RJA, RJC, RJF, RJH, RJI, RJM, RJN, RJU, SKA		
Rascasse	BBS, RSE, SCO , SCS		
Rémora	HTL		
Requin	ALV, BSH, CCE, DGH, DGS, DGX, GAG, GAM, QUB, SBL, SCK, SDV, SKH, SMA		
Rouget	MUR, MUT, MUX, RPY		
Roussette	SCL, SYC, SYT		
Sabre	BSF, SFS		
Sagre	ETX		
Saint Pierre	JOD		
Sandre	FPP		
Sanglier	BOC		
Sar	CTB, SBZ, SHR, SRG, SWA		
Sardine	PIL		
Sardinelle	SAA		
Saumon	SAL		
Saupe	SLM		
Sebaste	BRF, RED, TJX		
Seiche	CTC, CTL, EJE		

Annex V: Description of the datasets DB_CoAct and DB_Trawl

Variable	Description
SOURCE	Data source HALIOP or SACROIS
NAVS_COD_ANO	Vessel identification code
LONGUEUR_LHT	Length overall of the vessel
CAT_TAILLE	Category of length overall of the vessel (less than 10 meters, between 10 and 12 meters, between 12 and 15 meters, between 15 and 18 meters, more than 18 meters)
NAVP_JAUGE_GT	Vessel gauge
NAVP_PUISSANCE_AD	Power of the vessel
ENGIN_FAO_PRINC_COD	Main gear used by the vessel according to the European vessel registry
ENGIN_FAO_SEC_COD	Secondary gear used by the vessel according to the European vessel registry
ANNEE	Year of the fishing date
MOIS	Month of the fishing date
JOUR	Day of the fishing date
ESPECE_COD_FAO	FAO code of the species fished
GROUPE_ESP	Species group
ENGIN_SACROIS_COD	Fishing gear used
CAT_ENGIN	Category of fishing gear used
LATITUDE	Latitude of the centroïde of the square33 where fishing took place
LONGITUDE	Longitude of the centroïde of the square33 where fishing took place
CARRE_33	Identification number of the square33
EFFORT_JBAT / TEMPS_PECHE_H	Fishing effort in day (CoAct) or hour (dataChal)
QUANT_POIDS_VIF_KG	Quantity fished in kilograms
LPUE	Catch-per-unit-effort
LPUE_STD	Standardised LPUE
MONTANT_EUOS	Value in euros
VPUE	Value-per-unit-effort
VPUE_STD	Standardised VPUE

Annex VI: Percentage of vessels on which we have information compared to the ones in the European vessel registry by year and gear groups

YEAR	G	FPO	LL	PS
2015	1,5	20,0	2,9	28,6
2016	1,3	15,8	2,6	28,6
2017	0,5	4,9	3,4	26,3
2018	0,6	8,3	3,1	23,7
2019	0,4	2,9	3,1	8,1
2020	0,2	1,5	3,5	13,5
2021	0,5	8,0	7,1	17,9
2022	1,5	19,7	8,4	24,3
2023	3,0	20,2	8,0	23,7
2024	3,0	17,0	7,5	23,7
Mean	**1,3**	**11,8**	**5,0**	**21,8**

Annex VII: Quantity of fishing trips where the species (group) was fished for nets (G) and traps (FPO). The species groups described by less than 50 fishing trips on the entire study period are in orange, the one described by more in green.

Species group (French name)	Species group (English name)	G	FPO
Bar	Sea bass	520	
Barbue	Brill	559	
Baudroie	Monkfish	1040	55
Capelan	Capelin	236	
Chinchard	Horse mackerel	350	
Congre	European conger	72	205
Dorade royale	Gilt-head bream	702	
Grondin	Gurnard	581	
Langoustes et homards	Lobster	389	28
Maquereau	Mackerel	1013	
Merlu	Hake	1793	100
Mulet	Mullet	328	
Pageot	Pandora	1090	
Poulpe	Octopus	549	1707
Raie	Rays	654	94
Rascasse	Scorpionfish	319	
Rouget	Goatfish	575	
Roussette	Catshark	130	
Seiche	Cuttlefish	451	134
Sole	Sole	1383	90
Turbot	Turbot	238	

Annex VIII: References and models selected for the standardisation of LPUE and VPUE. The references were chosen according to the studies of Mignuccci (2021); Morfin et al. (2012); Morfin et al. (2016); Vaz et al. (2023) and also according to the data available

Variable	Gear	Species	Year	Month	Season	Model selected	Distribution
LPUE	G	Sea bass	2023	2	winter	log(LPUE) ~ ANNEE + MOIS + CARRE_33	Gaussian
LPUE	G	Brill	2023	2	winter	log(LPUE) ~ ANNEE + MOIS + CARRE_33	Gaussian
LPUE	G	Monkfish	2023	6	summer	LPUE ~ ANNEE + MOIS + CARRE_33	Gamma : link = log
LPUE	G	Capelin	2020	8	summer	log(LPUE) ~ MOIS + CARRE_33	Gaussian
LPUE	G	Horse mackerel	2023	4	summer	LPUE ~ ANNEE + MOIS + CARRE_33	Gamma : link = log
LPUE	G	European conger	2022	12	winter	log(LPUE) ~ MOIS + CARRE_33	Gaussian
LPUE	G	Gilt-head bream	2023	10	winter	LPUE ~ ANNEE + MOIS + CARRE_33	Gamma : link = log
LPUE	G	Gurnard	2024	6	summer	LPUE ~ ANNEE + MOIS + CARRE_33	Gamma : link = log
LPUE	G	Lobster	2023	6	summer	LPUE ~ MOIS + CARRE_33	Gamma : link = log
LPUE	G	Mackerel	2023	2	winter	log(LPUE) ~ ANNEE + MOIS + CARRE_33	Gaussian
LPUE	G	Hake	2023	6	summer	LPUE ~ ANNEE + MOIS + CARRE_33	Gamma : link = log
LPUE	G	Mullet	2023	10	winter	log(LPUE) ~ ANNEE + MOIS + CARRE_33	Gaussian
LPUE	G	Pandora	2023	4	summer	LPUE ~ ANNEE + MOIS + CARRE_33	Gamma : link = log
LPUE	G	Octopus	2023	6	summer	LPUE ~ ANNEE + MOIS + CARRE_33	Gamma : link = log
LPUE	G	Rays	2023	6	summer	LPUE ~ ANNEE + MOIS + CARRE_33	Gamma : link = log
LPUE	G	Scorpionfish	2023	6	summer	LPUE ~ ANNEE + MOIS + CARRE_33	Gamma : link = log
LPUE	G	Goatfish	2023	3	winter	LPUE ~ MOIS + CARRE_33	Gamma : link = log
LPUE	G	Catshark	2018	6	summer	LPUE ~ MOIS + CARRE_33	Gamma : link = log
LPUE	G	Cuttlefish	2023	5	summer	LPUE ~ ANNEE + MOIS + CARRE_33	Gamma : link = log
LPUE	G	Sole	2023	2	winter	LPUE ~ ANNEE + MOIS + CARRE_33	Gamma : link = log
LPUE	G	Turbot	2023	2	winter	LPUE ~ MOIS + CARRE_33	Gamma : link = log

LPUE	FPO	Monkfish	2023	6	summer	LPUE ~ MOIS + CARRE_33	Gamma : link = log
LPUE	FPO	European conger	2023	12	winter	LPUE ~ ANNEE + CARRE_33	Gamma : link = log
LPUE	FPO	Lobster	2022	6	summer	LPUE ~ MOIS + CARRE_33	Gamma : link = log
LPUE	FPO	Hake	2023	6	summer	LPUE ~ ANNEE + MOIS + CARRE_33	Gamma : link = log
LPUE	FPO	Octopus	2023	6	summer	LPUE ~ ANNEE + MOIS + CARRE_33	Gamma : link = log
LPUE	FPO	Rays	2023	6	summer	LPUE ~ MOIS + CARRE_33	Gamma : link = log
LPUE	FPO	Cuttlefish	2023	5	summer	LPUE ~ ANNEE + CARRE_33	Gamma : link = log
LPUE	FPO	Sole	2023	2	winter	LPUE ~ ANNEE + MOIS + CARRE_33	Gamma : link = log
LPUE	OTB	Sea bass	2023	2	winter	log(LPUE) ~ ANNEE + MOIS + NAVS_COD_ANO	Gaussian
LPUE	OTB	Brill	2023	2	winter	LPUE ~ ANNEE + MOIS + NAVS_COD_ANO	Gamma : link = log
LPUE	OTB	Monkfish	2023	6	summer	LPUE ~ ANNEE + MOIS + NAVS_COD_ANO	Gamma : link = log
LPUE	OTB	Capelin	2023	8	summer	LPUE ~ ANNEE + MOIS + NAVS_COD_ANO	Gamma : link = log
LPUE	OTB	European conger	2023	12	winter	log(LPUE) ~ ANNEE + MOIS + NAVS_COD_ANO	Gaussian
LPUE	OTB	Gilt-head bream	2023	10	winter	log(LPUE) ~ ANNEE + MOIS + NAVS_COD_ANO	Gaussian
LPUE	OTB	Gurnard	2023	6	summer	LPUE ~ ANNEE + MOIS + NAVS_COD_ANO	Gamma : link = log
LPUE	OTB	Lobster	2023	6	summer	LPUE ~ ANNEE + MOIS + NAVS_COD_ANO	Gamma : link = log
LPUE	OTB	Hake	2023	6	summer	log(LPUE) ~ ANNEE + MOIS + NAVS_COD_ANO	Gaussian
LPUE	OTB	Mullet	2023	10	winter	log(LPUE) ~ ANNEE + MOIS + NAVS_COD_ANO	Gaussian
LPUE	OTB	Pandora	2023	4	summer	log(LPUE) ~ ANNEE + MOIS + NAVS_COD_ANO	Gaussian
LPUE	OTB	Octopus	2023	6	summer	LPUE ~ ANNEE + MOIS + NAVS_COD_ANO	Gamma : link = log
LPUE	OTB	Rays	2023	6	summer	log(LPUE) ~ ANNEE + MOIS + NAVS_COD_ANO	Gaussian
LPUE	OTB	Scorpionfish	2023	6	summer	LPUE ~ ANNEE + MOIS + NAVS_COD_ANO	Gamma : link = log
LPUE	OTB	Goatfish	2023	3	winter	log(LPUE) ~ ANNEE + MOIS + NAVS_COD_ANO	Gaussian

LPUE	OTB	Catshark	2023	6	summer	LPUE ~ ANNEE + MOIS + NAVS_COD_ANO	Gamma : link = log
LPUE	OTB	Cuttlefish	2023	5	summer	log(LPUE) ~ ANNEE + MOIS + NAVS_COD_ANO	Gaussian
LPUE	OTB	Sole	2023	2	winter	LPUE ~ ANNEE + MOIS + NAVS_COD_ANO	Gamma : link = log
LPUE	OTB	Turbot	2023	2	winter	LPUE ~ ANNEE + MOIS + NAVS_COD_ANO	Gamma : link = log
LPUE	OTM	Horse mackerel	2023	4	summer	log(LPUE) ~ ANNEE + MOIS + NAVS_COD_ANO	Gaussian
LPUE	OTM	Mackerel	2023	2	winter	log(LPUE) ~ ANNEE + MOIS + NAVS_COD_ANO	Gaussian
VPUE	G	All	2023	6	summer	VPUE ~ ANNEE + MOIS + CARRE_33	Gamma : link = log
VPUE	FPO	All	2023	6	summer	VPUE ~ ANNEE + MOIS + CARRE_34	Gamma : link = log

Annex IX: Standardisation results: A: graph of coefficient with their confidence intervals, only the coefficient whose confidence interval do not include zero were used. B: Standardized values versus observations

LPUE net-monkfish

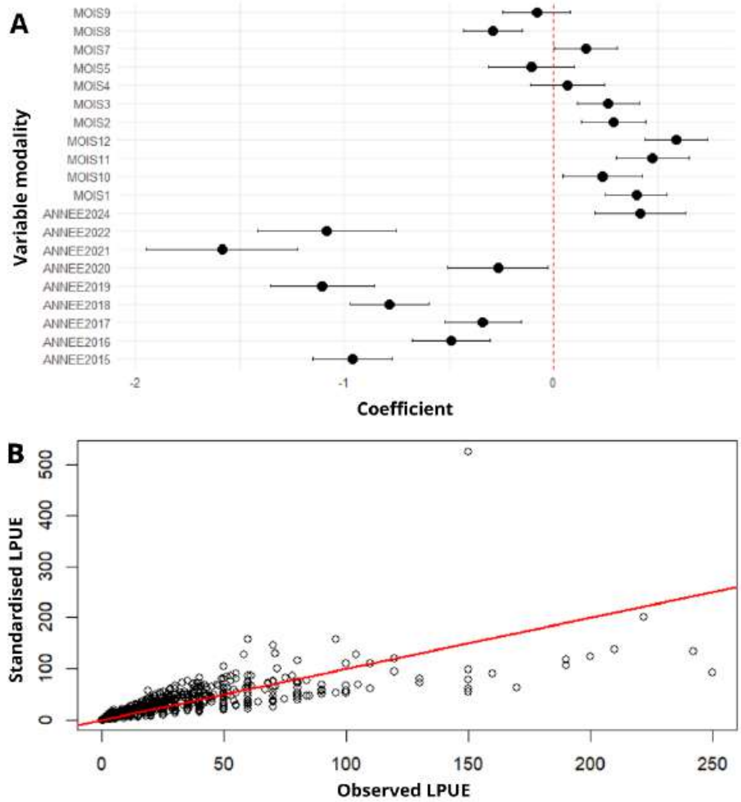

LPUE net-hake

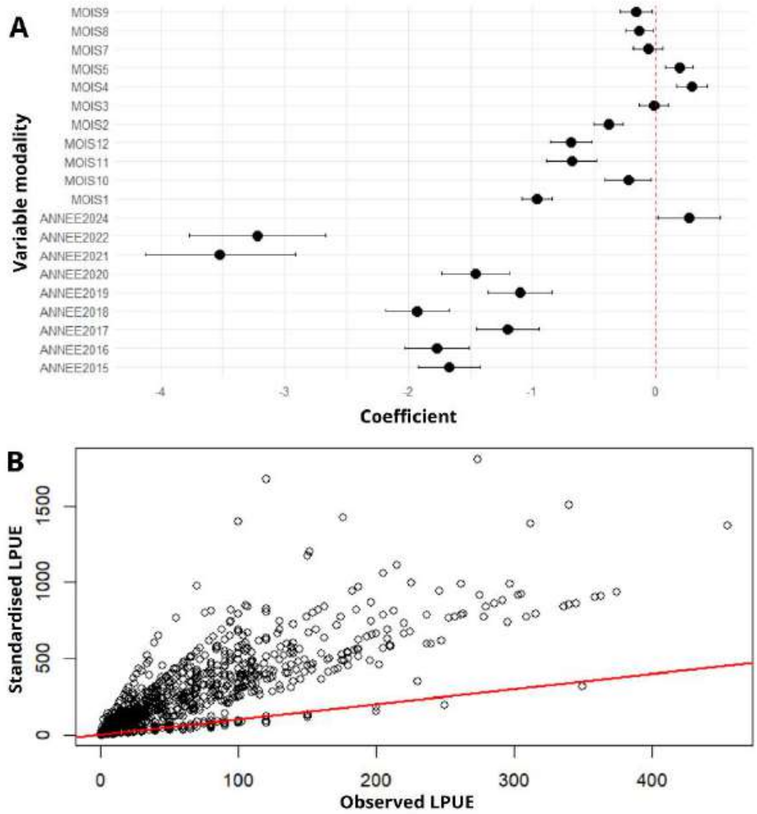

LPUE net-sole

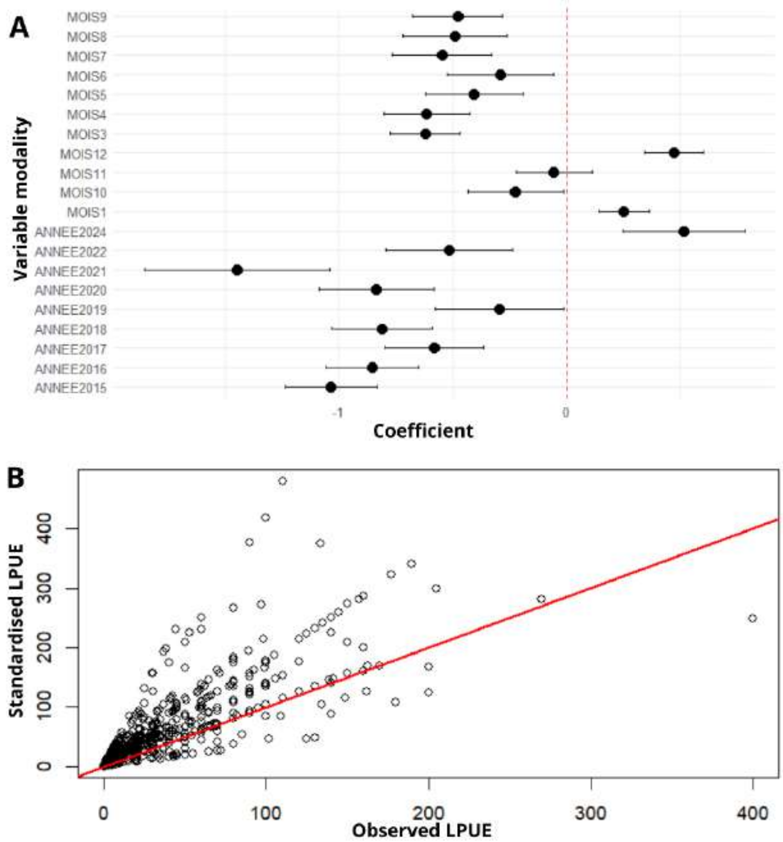

LPUE trap-octopus

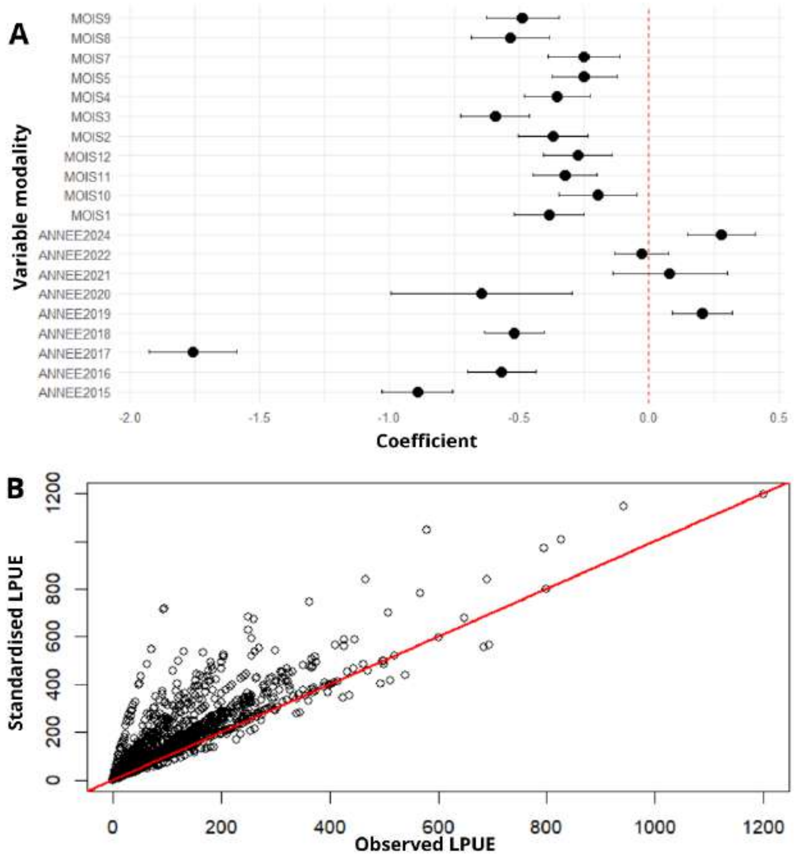

VPUE net

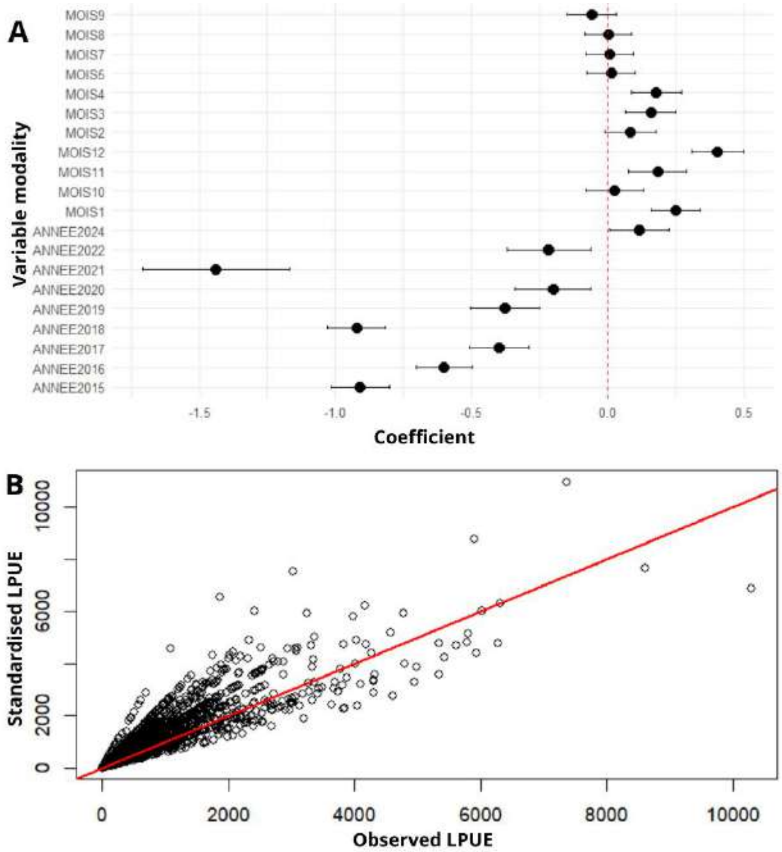

VPUE trap

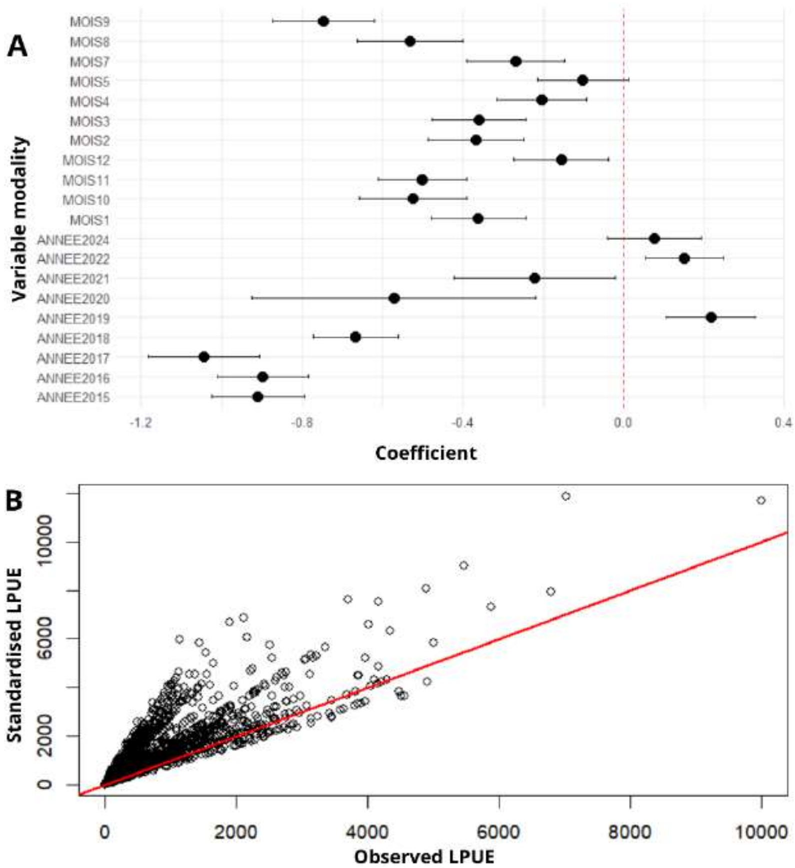

Annex X: Characteristics of the variograms models used for the estimation of LPUE and VPUE through kriging (first table) and cokriging (second table), and for the models used to explore seasonal variability (third table)

Model	Nugget	Spherical sill	Spherical range	Linear slope
OK G Monkfish mean	NA	5552.935	0.305	NA
OK G Hake mean	NA	14244.895	0.161	10442.851
OK G Sole mean	NA	2244.604	0.306	2215.125
OK FPO Octopus mean	6131.412	5400.465	0.245	11531.877
OK G Monkfish jitter	NA	1436.185	0.438	202.367
OK G Hake jitter	57171.577	NA	NA	2895.434
OK G Sole jitter	1699.100	1945.687	0.192	1403.927
OK FPO Octopus jitter	10901.268	10278.383	0.188	NA
OK G VPUE mean	102237.943	389935.454	0.335	257586.750
OK G VPUE jitter	307711.747	117676.701	0.168	79535.391
OK FPO VPUE mean	218190.070	610795.103	0.182	363744.058
OK FPO VPUE jitter	827613.134	674730.771	0.217	1502343.906

COK LPUE G OT Monkfish mean	
Nugget	$\begin{bmatrix} 1046.179 & \\ -10.902 & 0.114 \end{bmatrix}$
Spherical sill	$\begin{bmatrix} 4588.615 & \\ 48.754 & 16.164 \end{bmatrix}$
Spherical range	0.392
Linear slope	NA
COK LPUE G OT Hake mean	
Nugget	$\begin{bmatrix} 11074.360 & \\ 9.335 & 2.914 \end{bmatrix}$
Spherical sill	$\begin{bmatrix} 3239.918 & \\ 12.493 & 5.223 \end{bmatrix}$
Spherical range	0.468
Linear slope	$\begin{bmatrix} 10244.930 & \\ -11.839 & 5.133 \end{bmatrix}$
COK LPUE G OT Sole mean	
Nugget	NA
Spherical sill	$\begin{bmatrix} 2302.399 & \\ -1.696 & 0.020 \end{bmatrix}$
Spherical range	0.330
Linear slope	$\begin{bmatrix} 2165.109 & \\ 7.759 & 0.028 \end{bmatrix}$
COK LPUE FPO OT Octopus mean	
Nugget	$\begin{bmatrix} 9952.656 & \\ -6.270 & 0.432 \end{bmatrix}$
Spherical sill	$\begin{bmatrix} 82182.032 & \\ 653.495 & 43.173 \end{bmatrix}$
Spherical range	50.895
Linear slope	NA

Model	Nugget	Spherical sill	Spherical range	Linear slope
OK VPUE G mean T1	NA	531920.575	0.188	812639.986
OK VPUE G mean T2	335366.956	497799.351	1.327	52268.584
OK VPUE G mean T3	NA	1270037.736	0.500	1270037.736
OK VPUE G mean T4	553643.283	NA	NA	NA
OK VPUE FPO mean T1	NA	1330258.047	0.211	NA
OK VPUE FPO mean T2	15147.300	160325.041	0.152	39866.434
OK VPUE FPO mean T3	NA	632949.676	0.260	229727.665
OK VPUE FPO mean T4	119378.218	753841.059	0.337	NA

Annex XI: Results of the cokriging estimations for net-monkfish, net-hake, net-sole, and trap-octopus using LPUE from other species fished by the same gear as covariables

Variography

COK LPUE G Monkfish species mean

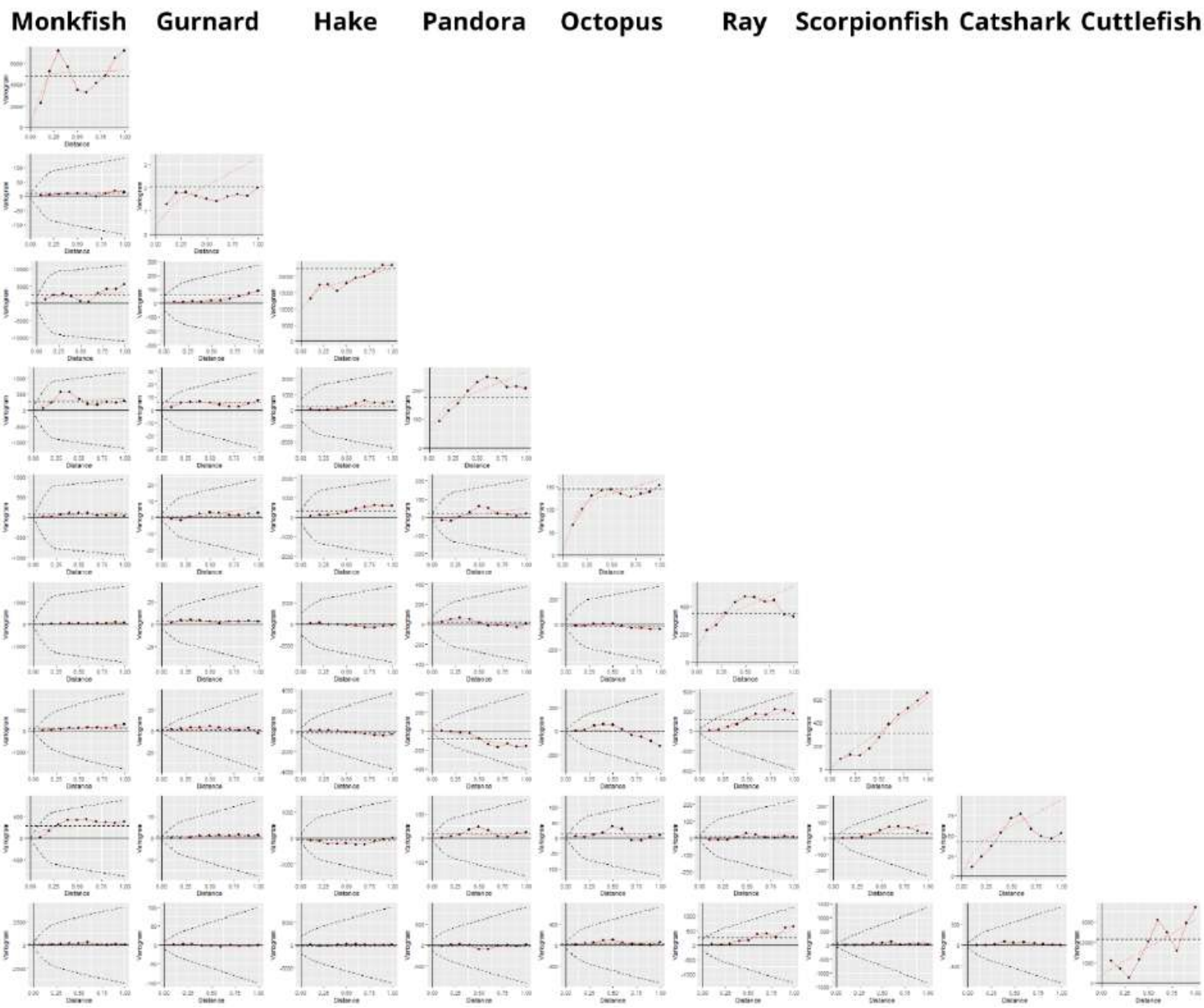

Model	COK LPUE G Monkfish species mean
Nugget	$\begin{bmatrix} 7.612 & & & & & & & & \\ 0.132 & 0.298 & & & & & & & \\ 229.679 & 13.926 & 9634.816 & & & & & & \\ -6.293 & 1.076 & 125.696 & 53.370 & & & & & \\ 4.082 & 0.206 & 38.802 & -18.675 & 9.797 & & & & \\ 2.880 & -2.786 & 115.105 & 7.981 & -17.475 & 98.190 & & & \\ -2.347 & 1.081 & 21.680 & 16.368 & -2.064 & -21.658 & 11.286 & & \\ 2.531 & 0.038 & 51.319 & -3.215 & 1.751 & -1.173 & -0.284 & 1.457 & \\ -6.156 & 1.438 & 161.585 & -16.938 & 17.644 & -48.346 & -3.497 & -14.854 & 395.791 \end{bmatrix}$

Spherical sill	$\begin{bmatrix} 4998.586 & & & & & & & & \\ 0.368 & 0.623 & & & & & & & \\ 1325.731 & -24.076 & 4958.782 & & & & & & \\ 278.189 & 5.475 & -266.134 & 75.514 & & & & & \\ -2.820 & -2.544 & -92.413 & 8.004 & 92.807 & & & & \\ 11.717 & 6.632 & 46.968 & 69.123 & 21.167 & 151.599 & & & \\ 99.978 & -1.739 & 200.334 & -3.945 & 30.505 & 15.838 & 21.501 & & \\ 182.235 & 0.854 & -258.279 & 25.402 & 5.575 & -17.622 & -8.669 & 28.600 & \\ 52.119 & 0.977 & -301.646 & 20.051 & 7.114 & -15.211 & -11.026 & 24.183 & 23.232 \end{bmatrix}$
Spherical range	0.244
Linear slope	$\begin{bmatrix} 379.894 & & & & & & & & \\ 16.999 & 2.364 & & & & & & & \\ 1555.12 & 70.708 & 8179.603 & & & & & & \\ 90.163 & -2.006 & 757.245 & 135.353 & & & & & \\ 133.311 & 8.013 & 708.735 & 58.327 & 64.083 & & & & \\ 30.564 & -0.498 & -453.623 & -120.826 & -37.596 & 296.483 & & & \\ 77.839 & 6.845 & -642.580 & -191.274 & -53.144 & 334.239 & 576.803 & & \\ 75.324 & -0.595 & 96.677 & -15.207 & 1.272 & 47.266 & 96.647 & 63.39 & \\ 152.196 & -5.997 & 389.087 & -54.528 & 41.708 & 571.704 & 114.291 & 4.964 & 2672.51 \end{bmatrix}$

COK LPUE G Hake species mean

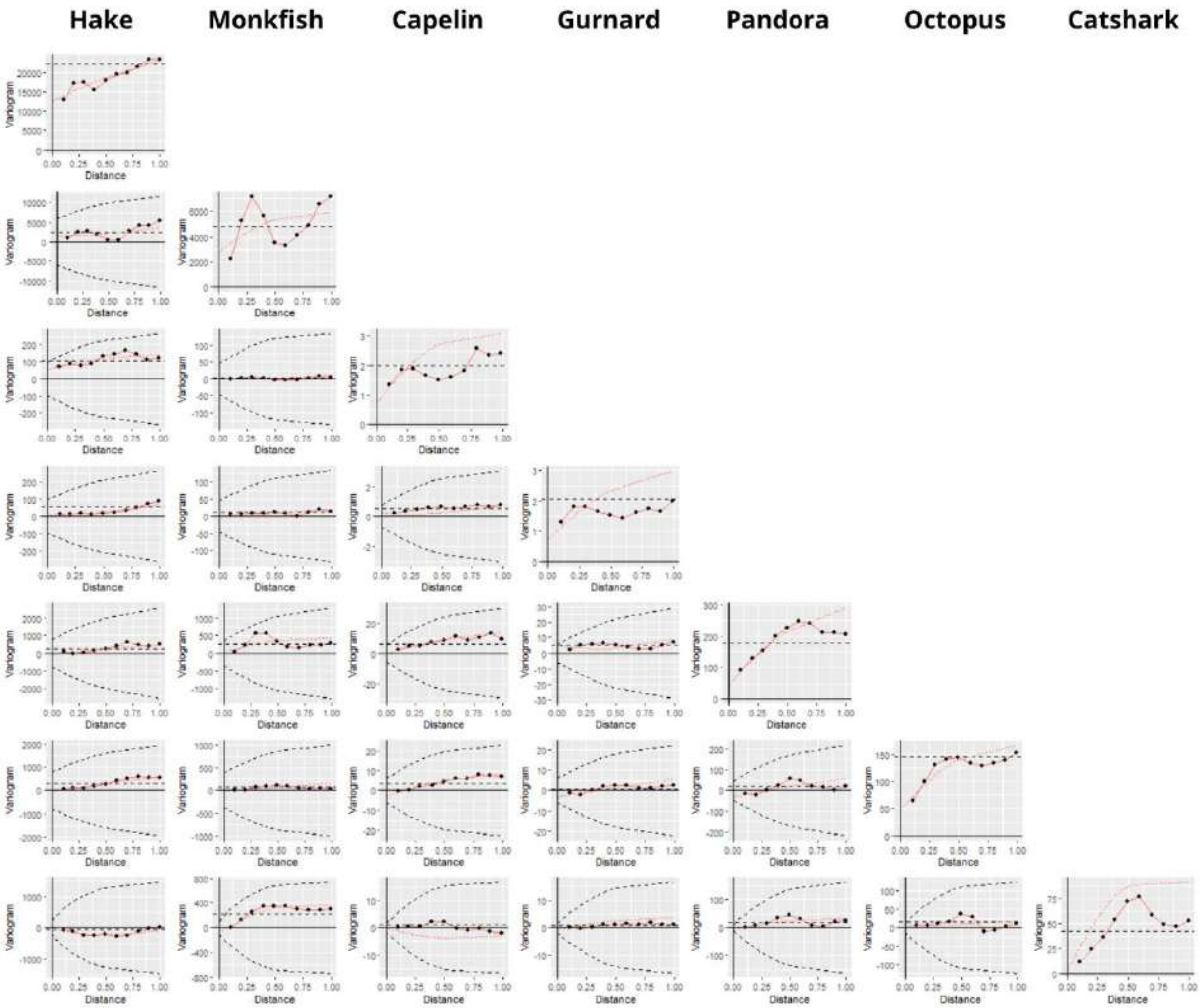

Model	COK LPUE G Hake species mean
Nugget	$\begin{bmatrix} 12702.854 & & & & & & \\ 1524.004 & 2816.920 & & & & & \\ 55.969 & 0.720 & 0.730 & & & & \\ 3.236 & 4.050 & 0.152 & 0.731 & & & \\ -70.086 & 29.152 & -0.333 & 5.082 & 45.375 & & \\ -44.413 & -10.330 & -2.675 & -3.046 & -31.101 & 48.945 & \\ -25.013 & -74.175 & -0.055 & -0.553 & -5.177 & 4.561 & 2.454 \end{bmatrix}$
Spherical sill	$\begin{bmatrix} 1586.487 & & & & & & \\ -996.959 & 1984.486 & & & & & \\ 32.321 & -9.131 & 1.668 & & & & \\ -24.285 & -10.623 & -0.431 & 0.963 & & & \\ 95.451 & 285.172 & 4.957 & -7.941 & 93.657 & & \\ 64.672 & -13.733 & 4.757 & 0.310 & 14.104 & 63.677 & \\ -313.061 & 360.887 & -4.582 & 1.883 & 23.253 & -2.938 & 82.346 \end{bmatrix}$
Spherical range	0.563
Linear slope	$\begin{bmatrix} 8941.378 & & & & & & \\ 3103.451 & 1093.177 & & & & & \\ 61.116 & 19.084 & 0.701 & & & & \\ 85.720 & 26.994 & 0.953 & 1.297 & & & \\ 473.532 & 119.313 & 9.227 & 12.304 & 151.856 & & \\ 589.042 & 188.710 & 6.119 & 8.360 & 75.496 & 54.285 & \\ 236.558 & 81.089 & 1.752 & 2.443 & 15.391 & 16.584 & 6.323 \end{bmatrix}$

COK LPUE G Sole species mean

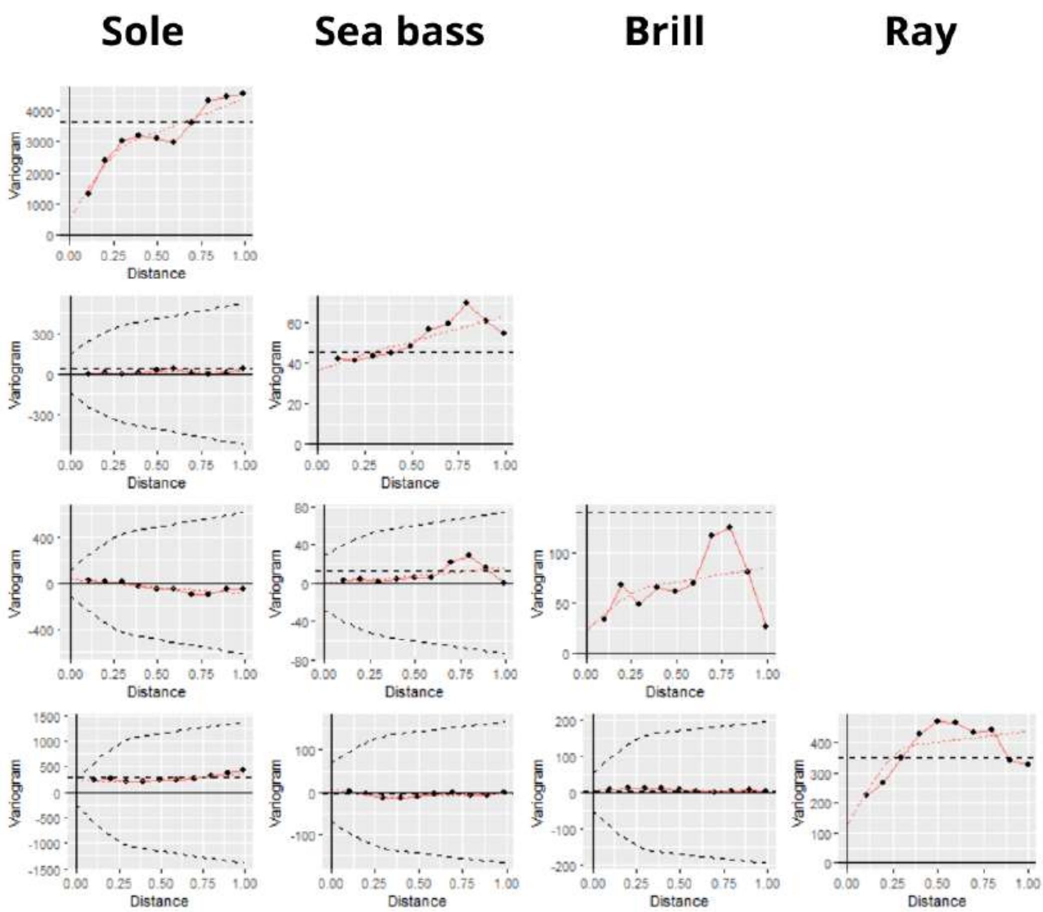

Model	COK LPUE G Sole species mean
Nugget	$\begin{bmatrix} 510.126 & & & \\ -3.385 & 36.702 & & \\ 35.851 & 1.050 & 21.733 & \\ 242.160 & 7.341 & 7.746 & 121.932 \end{bmatrix}$
Spherical sill	$\begin{bmatrix} 1738.703 & & & \\ 7.091 & 2.031 & & \\ -12.650 & -2.526 & 35.124 & \\ -92.497 & -21.572 & 4.502 & 244.946 \end{bmatrix}$
Spherical range	0.363
Linear slope	$\begin{bmatrix} 2153.367 & & & \\ 17.803 & 24.768 & & \\ -115.795 & 17.839 & 29.411 & \\ 201.491 & 10.698 & -11.954 & 71.567 \end{bmatrix}$

COK LPUE FPO Octopus species mean

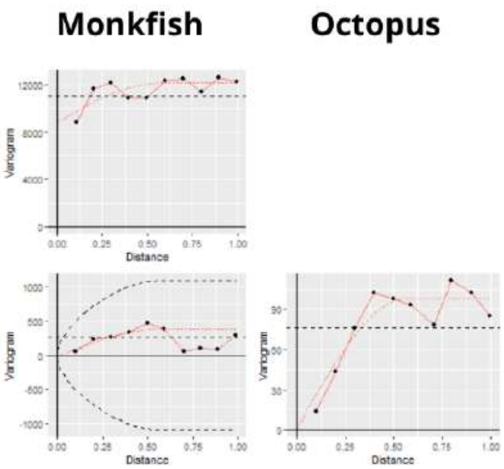

Model	COK LPUE FPO Octopus species mean
Nugget	$\begin{bmatrix} 8826.175 & \\ -18.271 & 0.038 \end{bmatrix}$
Spherical sill	$\begin{bmatrix} 3310.265 & \\ 402.675 & 98.079 \end{bmatrix}$
Spherical range	0.565
Linear slope	NA

Maps of LPUE estimates and standard deviation, they should be considered with caution (orange outline)

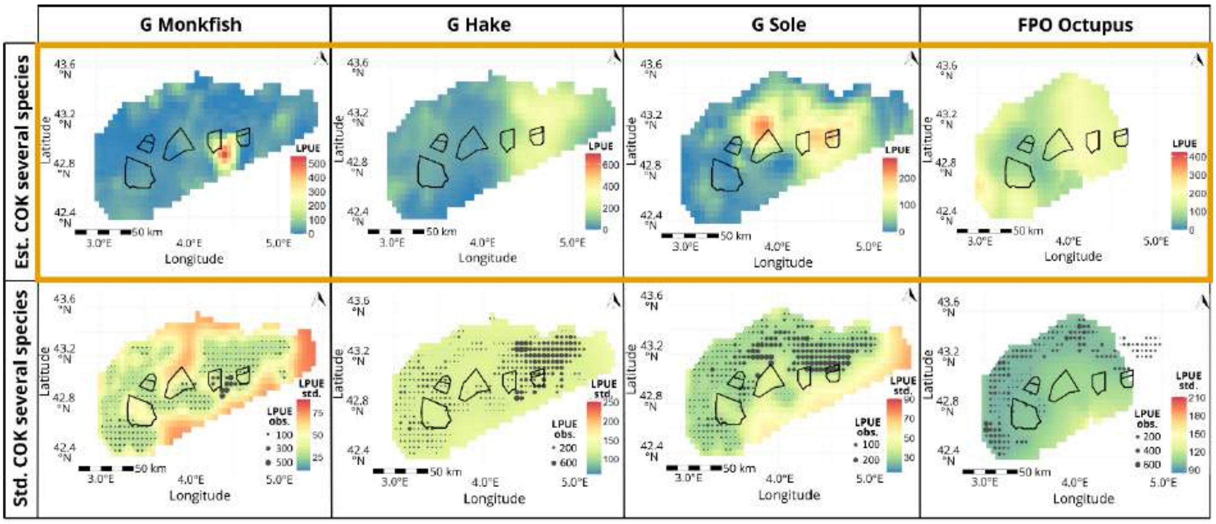

Cross-validation

Model	Mean prediction error	Mean squared prediction error	Mean standardized error
COK species G Monkfish mean	-0.44	1024	0.72
COK species G Hake mean	0.94	10716	0.76
COK species G Sole mean	-0.11	786	0.76
COK species FPO Octupus mean	-2.52	9522	0.96

L'INSTITUT agro Rennes Angers	Diplôme : Ingénieur agronome Spécialité : Sciences Halieutiques et Aquacoles Spécialisation / option : Ecologie halieutique Enseignant référent : Olivier Le Pape
Auteur(s) : Louise DANIEL Date de naissance : 18/04/2001	Organisme d'accueil : UMR Marbec Station Ifremer de Sète Adresse : Boulevard Jean Monnet, CS 30171, 34203 Sète Cedex
Nb pages : 63 Annexe(s) : 11	
Année de soutenance : 2025	Maître de stage : Stéphanie MAHEVAS

Titre français : Étude prospective des débarquements potentiels associés à la co-activité entre pêche et parcs éoliens offshores dans le golfe du Lion

Titre anglais : A prospective study on the evolution of fisheries' landings through co-location with energy production in the offshore wind farms of the Gulf of Lion

Résumé :

Le développement de cinq parcs éoliens en mer (OWFs) dans le golfe du Lion d'ici 2050, entraînera l'interdiction d'accès de ces zones aux chalutiers. La filière de la pêche s'interroge sur la possibilité et la pertinence de mettre en place des co-activités de pêche dans les parcs avec d'autres engins comme les filets et les casiers-pots (projet Fishwind). Ce mémoire vise à réaliser des estimations des débarquements potentiels en volume et en valeur, que pourraient réaliser des pêcheurs avec ces engins dans ces zones. En utilisant des bases de données spatialisées de l'Ifremer (SIH-SACROIS) et de l'OP SATHOAN (HALIOP), des modèles de krigeage et de cokrigeage ont permis de produire des cartes de distribution à l'échelle du golfe du Lion des débarquements par unité d'effort (LPUE) et des valeurs par unité d'effort (VPUE), ainsi que des estimations avec des enveloppes d'incertitude dans chacun des parcs. Pour les filets, les résultats révèlent que des débarquements significativement plus importants en poids seraient possibles pour la baudroie, la sole, le merlu dans les trois parcs à l'est du golfe du Lion. Ces parcs offriraient aussi les meilleures opportunités économiques pour cet engin avec une variabilité saisonnières des VPUE présentant des valeurs maximales en été ou en hiver, selon les parcs. En revanche, les VPUE des casiers ou pots seraient semblables dans tous les parcs, resteraient stables d'une saison à l'autre. Ces résultats préliminaires, bien qu'encourageants, présentent des intervalles de confiance larges et doivent donc être interprétés avec précaution.

Abstract :

The development of five offshore wind farms (OWFs) in the Gulf of Lion by 2050 will result in trawlers being banned from these areas. The fishing industry is questioning the possibility and relevance of setting up a co-location between fishing and OWFs using other fishing gears such as nets and pots (Fishwind project). This master thesis aims to estimate the potential landings in weight and value that fishers could achieve with these fishing gears in these areas. Using spatial databases from Ifremer (SIH-SACROIS) and OP SATHOAN (HALIOP), kriging and cokriging models were used to produce maps of the distribution of landings per unit effort (LPUE) and values per unit effort (VPUE) across the Gulf of Lion, as well as estimates with confidence intervals in each OWF. For nets, the results reveal that significantly higher landings in weight would be possible for monkfish, sole and hake in the three wind farms to the east of the Gulf of Lion. These OWFs would also offer the best economic opportunities for this gear, with seasonal variability in VPUE showing maximum values in summer or winter, depending on the park. On the other hand, the VPUE for pots would be similar in all OWFs and remain stable from one season to the other. These preliminary results, although encouraging, have wide confidence intervals and should be interpreted with caution.

Mots-clés : co-activité, petite pêche, éolien en mer, cokrigeage, prédiction de capture et revenus, golfe du Lion

Key Words: co-location, small-scale fisheries, offshore windfarm, cokriging, landings predictions in weight and value, Gulf of Lion